

Article

Synthesis, Characterization and In Vitro Evaluation of Novel 5-Ene-thiazolo[3,2-*b*][1,2,4]triazole-6(5*H*)-ones as Possible Anticancer Agents

Serhii Holota ^{1,2,*} , Sergiy Komykhov ^{3,4}, Stepan Sysak ¹, Andrzej Gzella ⁵, Andriy Cherkas ^{6,†}  and Roman Lesyk ^{1,7,*} 

- ¹ Department of Pharmaceutical, Organic and Bioorganic Chemistry, Danylo Halytsky Lviv National Medical University, Pekarska 69, 79010 Lviv, Ukraine; stepansysak@pm.me
- ² Department of Organic Chemistry and Pharmacy, Lesya Ukrainka Volyn National University, Volya Avenue 13, 43025 Lutsk, Ukraine
- ³ State Scientific Institution "Institute for Single Crystals", National Academy of Sciences of Ukraine, Nauky Ave 60, 61072 Kharkiv, Ukraine
- ⁴ Applied Chemistry Department, Karazin Kharkiv National University, Svobody Sq. 4, 61022 Kharkiv, Ukraine
- ⁵ Department of Organic Chemistry, Poznan University of Medical Sciences, Grunwaldzka 6, 60-780 Poznan, Poland; akgzella@ump.edu.pl
- ⁶ Department of Internal Medicine #1, Danylo Halytsky Lviv National Medical University, Pekarska 69, 79010 Lviv, Ukraine; cherkasandriy@yahoo.com or andriy.cherkas@sanofi.com
- ⁷ Department of Public Health, Dietetics and Lifestyle Disorders, Faculty of Medicine, University of Information Technology and Management in Rzeszow, Sucharskiego 2, 35-225 Rzeszow, Poland
- * Correspondence: golota_serg@yahoo.com (S.H.); dr_r_lesyk@org.lviv.net (R.L.); Tel.: +380-97-226-00-66 (S.H.); +380-32-275-59-66 (R.L.)
- † Current address: Team Early Projects Type 1 Diabetes, Therapeutic Area Diabetes and Cardiovascular Medicine, Research & Development, Sanofi-Aventis Deutschland GmbH, Industriepark Höchst-H831, 65926 Frankfurt am Main, Germany.



Citation: Holota, S.; Komykhov, S.; Sysak, S.; Gzella, A.; Cherkas, A.; Lesyk, R. Synthesis, Characterization and In Vitro Evaluation of Novel 5-Ene-thiazolo[3,2-*b*][1,2,4]triazole-6(5*H*)-ones as Possible Anticancer Agents. *Molecules* **2021**, *26*, 1162. <https://doi.org/10.3390/molecules26041162>

Academic Editors: Beata Morak-Młodawska and Diego Muñoz-Torrero

Received: 10 February 2021

Accepted: 20 February 2021

Published: 22 February 2021

Publisher's Note: MDPI stays neutral with regard to jurisdictional claims in published maps and institutional affiliations.



Copyright: © 2021 by the authors. Licensee MDPI, Basel, Switzerland. This article is an open access article distributed under the terms and conditions of the Creative Commons Attribution (CC BY) license (<https://creativecommons.org/licenses/by/4.0/>).

Abstract: The present paper is devoted to the search for drug-like molecules with anticancer properties using the thiazolo[3,2-*b*][1,2,4]triazole-6-one scaffold. A series of 24 novel thiazolo-[3,2-*b*][1,2,4]triazole-6-ones with 5-aryl(heteryl)idene- and 5-aminomethylidene-moieties has been synthesized employing three-component and three-stage synthetic protocols. A mixture of *Z/E*-isomers was obtained in solution for the synthesized 5-aminomethylidene-thiazolo[3,2-*b*]-[1,2,4]triazole-6-ones. The compounds have been studied for their antitumor activity in the NCI 60 lines screen. Some compounds present excellent anticancer properties at 10 μM. Derivatives **2h** and **2i** were the most active against cancer cell lines without causing toxicity to normal somatic (HEK293) cells. A preliminary SAR study had been performed for the synthesized compounds.

Keywords: thiazolo[3,2-*b*][1,2,4]triazole-6(5*H*)-ones; multicomponent reactions; *Z/E*-isomers; anticancer activity; SAR

1. Introduction

We are currently witnessing a great progress in research and development of new anti-tumor therapeutic agents. Nevertheless, cancer remains the second most frequent cause of death in the world and the problem is far from being solved [1]. Cancer is a systemic disease and both its internal metabolic and genetic aberrations as well as the efficiency of immunologic protection play a role in tumor development and progression [2]. Chronic inflammation, redox imbalance, metabolic dysfunctions and altered glucose metabolism as well as many other endogenous and exogenous factors play roles in disease biology and define outcomes [3–5]. This heterogeneity of cancer requires the application of various approaches to prevention and treatment that may include application of specific small molecules interfering with altered metabolic pathways in cancers, modulation of immune

response to transformed cells and precision medicine [6–8]. Therefore, the search for novel small molecules capable to modulate selectively metabolic processes including redox regulation remains of significant scientific and practical importance.

The class of 5-ene-thiazolo[3,2-*b*][1,2,4]triazole-6(5*H*)-ones bicyclic heteroatom-rich compounds [9] containing a 1,2,4-triazole ring and an enone/chalcone system cross-conjugated through a sulfur atom in the molecule has recently attracted the attention of medicinal chemists due to its diverse biological activities. Some 5-ene-thiazolo[3,2-*b*][1,2,4]triazole-6(5*H*)-ones have been studied successfully as potential anti-inflammatory [10–14], analgesic [11,13], antimicrobial [15], antifungal [16], antioxidant [17], anticonvulsant [18,19], antihypertensive [20] and anti-aggregation agents [21] (Figure 1). It is worth mentioning that the structural transformation of the carboxylic group into a 5-ene-thiazolo[3,2-*b*][1,2,4]triazole-6(5*H*)-one moiety has been proposed as a bioisosteric replacement or structure optimization pathway for the synthesis of novel derivatives to keep the main pharmacological profile and to reduce/improve toxicity parameters and activity profiles [10,22–24].

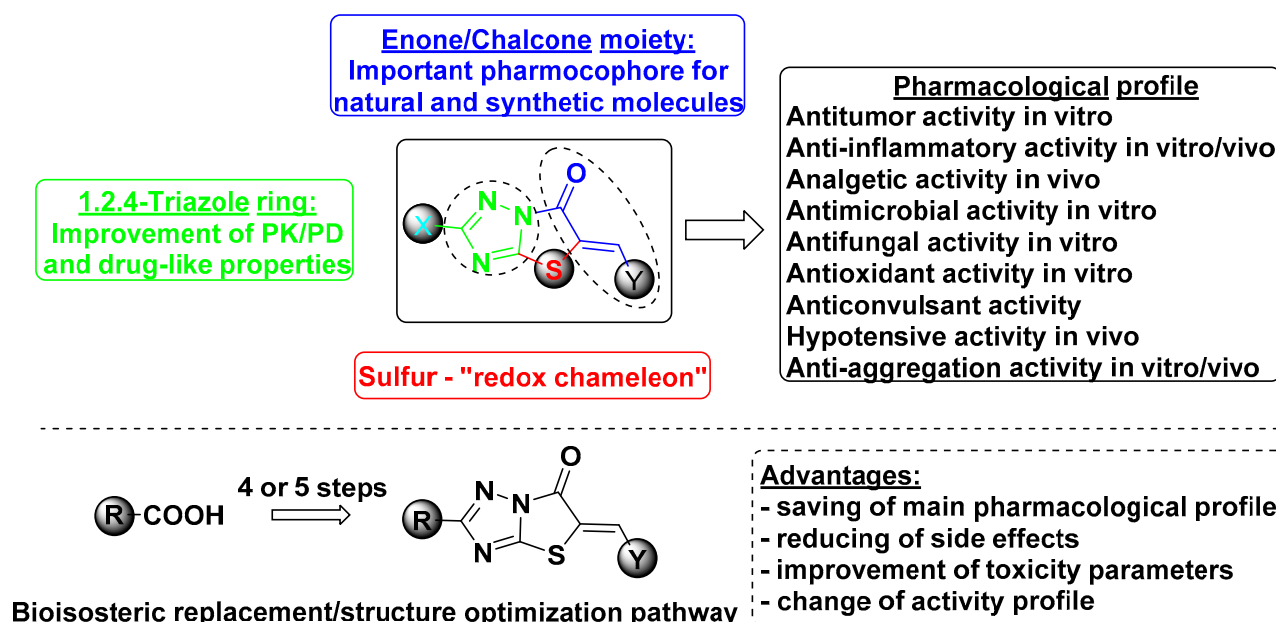


Figure 1. The current state of 5-ene-thiazolo[3,2-*b*][1,2,4]triazole-6(5*H*)-one bearing compounds in medicinal chemistry.

In addition to the abovementioned pharmacological features, some 5-ene-thiazolo[3,2-*b*][1,2,4]triazole-6(5*H*)-ones possess promising antitumor properties. A potential non-camptothecin topoisomerase 1 inhibitor (Top1) with the 5-ene-thiazolo[3,2-*b*][1,2,4]triazole-6(5*H*)-one scaffold (Figure 2A) had been identified using structure-based virtual screening and in vitro assays [25,26]. The mentioned compound at 10 μM showed superior Top1 inhibitory activity compared with the powerful natural Top1-inhibitor camptothecin. Using a similar screening approach the derivative CCT-196700 (Figure 2B) was identified and reported as a potential phospholipase C- γ 2 (PLC- γ 2) inhibitor with satisfactory activity parameters at 15 μM in the 3*H*-phosphatidylinositol 4,5-diphosphate biochemical and calcium release cell-based assays [27]. PLC- γ 2 is uniquely expressed in hematopoietic cells and considered a plausible target for the treatment of some cancer types [28]. 5-Ene-thiazolo[3,2-*b*][1,2,4]triazole-6(5*H*)-one derivatives (Figure 2C,D) with high impact on leukemia lines in the NCI-60 lines screening program were reported [29,30].

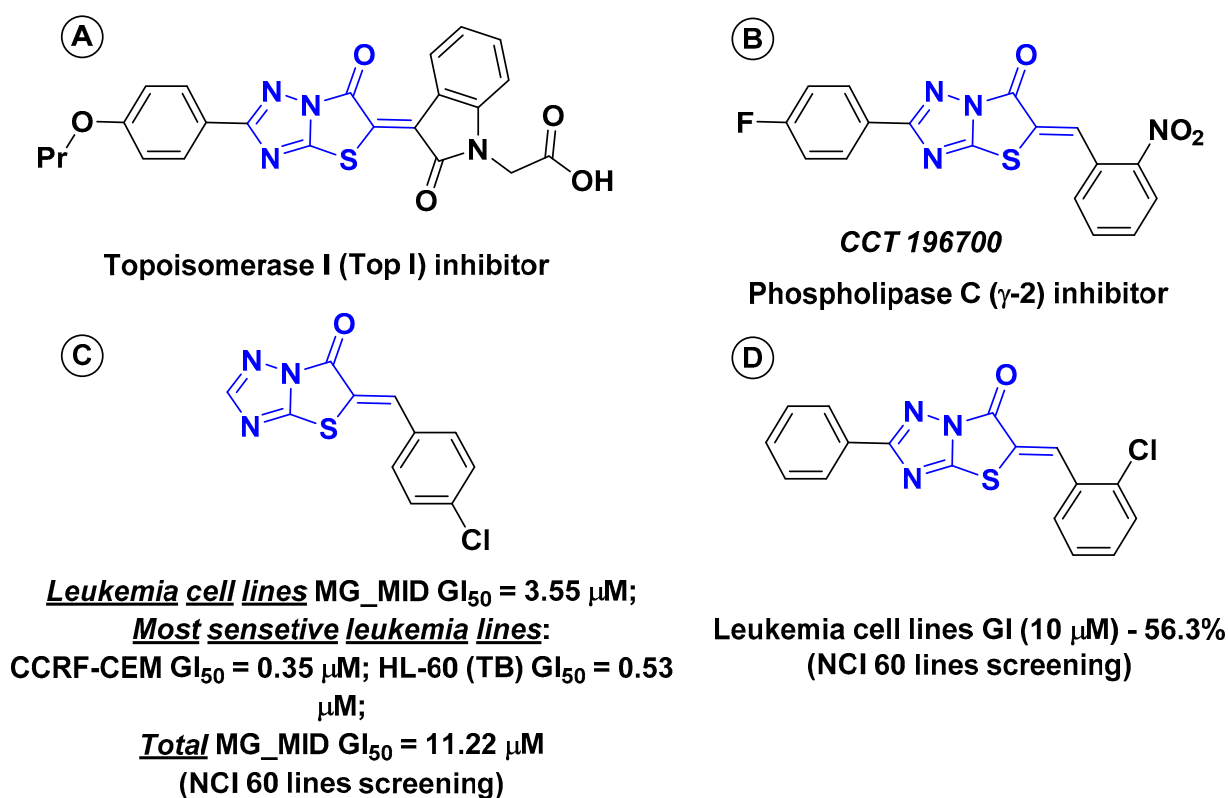


Figure 2. 5-Ene-thiazolo[3,2-*b*][1,2,4]triazole-6(5*H*)-ones with anticancer properties.

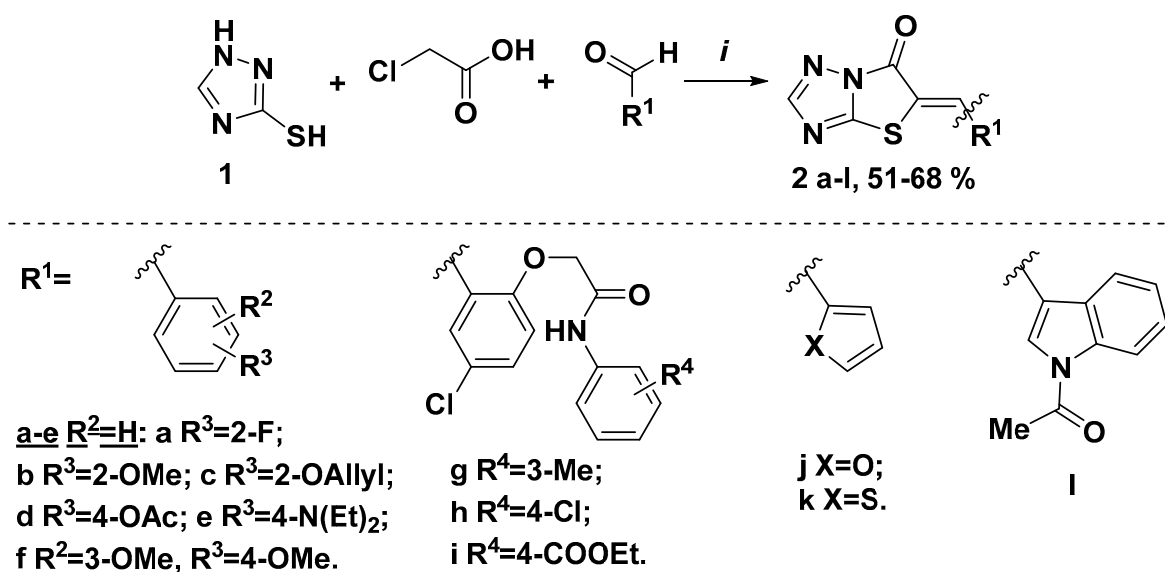
In view of our interest in the search for and study of new low-molecular heterocyclic modulators among thiazole-bearing molecules [31–34], herein, we report the synthesis, structure characterization and in vitro anticancer activity evaluation of some novel heterocyclic derivatives. This manuscript is intended to draw attention towards the chemistry and pharmacology of the 5-ene-thiazolo[3,2-*b*][1,2,4]triazole-6(5*H*)-one fragment and its further exploration as a prospective source of drug-like molecules.

2. Results and Discussion

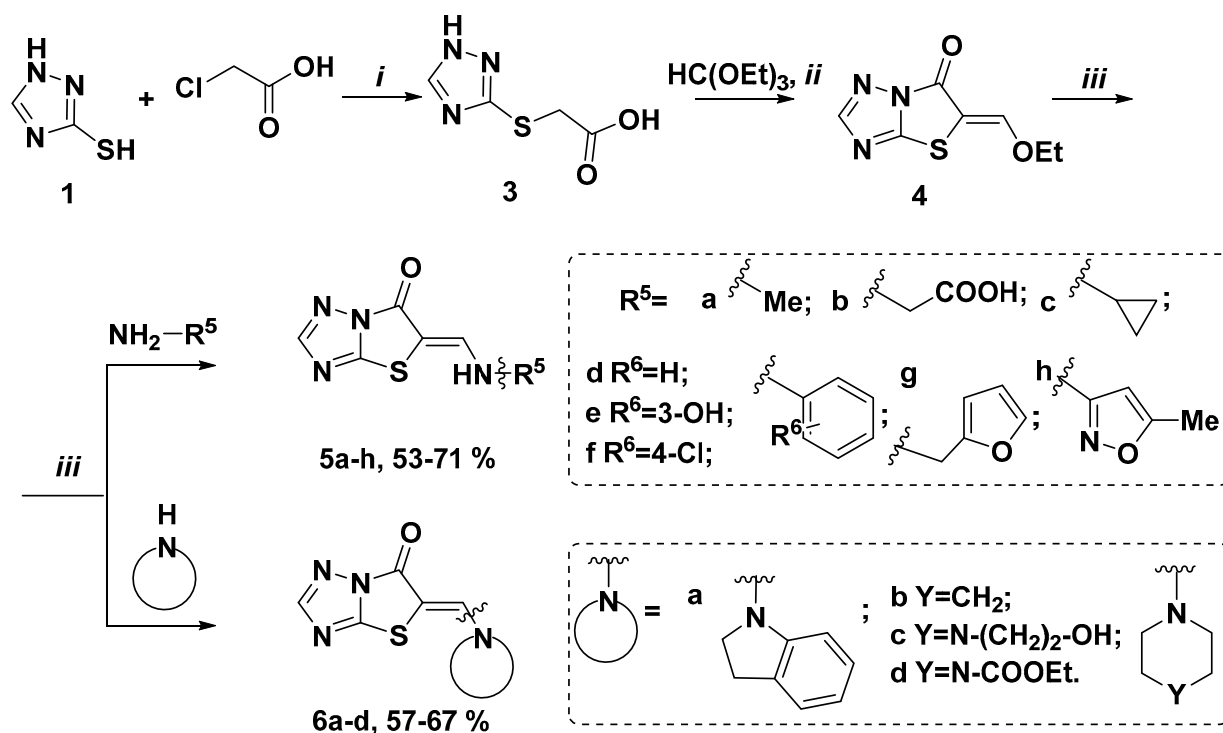
2.1. Chemical Synthesis

According to our synthetic goal and using the retrosynthetic approach, a multicomponent one-pot protocol [29] was employed for the synthesis of 5-aryl(heteryl)idene-derivatives **2a–l**. The reported data about the impact of substituents in position C-5 on pharmacological properties of thiazolo[3,2-*b*][1,2,4]triazole-6(5*H*)-ones and data from our study of anticancer activity with structure-activity relationships for this class of heterocyclic compounds [10–28] were the main reasons for the selection of the substituents R¹–R⁶. Thereby, by the three-component reaction of **1** with chloroacetic acid and aromatic/heteroaromatic aldehydes in a mixture AcONa + AcOH:Ac₂O employing convenient heating resulted in compounds **2a–l** (Scheme 1) which were purified by recrystallization.

The three-step approach was exploited for the preparation of 5-aminomethylidene-thiazolo[3,2-*b*][1,2,4]triazole-6(5*H*)-ones **5a–h**, **6a–d** (Scheme 2). Initially the 5-etoxy-methylidene derivative **4** was synthesized from **1** based on a published protocol [35]. The aminolysis of **4** by primary or secondary aliphatic/aromatic/heterocyclic amines in an alcoholic medium led to the formation of target derivatives **5a–h**, **6a–d**. The compounds were obtained in satisfactory yields and were recrystallized for purification (Scheme 2).



Scheme 1. Three-component synthesis of 5-aryl(heteryl)idene-thiazolo[3,2-*b*][1,2,4]triazole-6(5*H*)-ones (**2a-l**). Reagents and conditions: *i*) **1** (10 mmol), ClCH₂COOH (10 mmol), R^1 -CHO (12 mmol), AcONa (20 mmol), AcOH:Ac₂O (5 + 5 mL), reflux, 3 h.



Scheme 2. Synthesis of 5-aminomethylidene-thiazolo[3,2-*b*][1,2,4]triazole-6(5*H*)-ones **5a-h**, **6a-d**. Reagents and conditions: *i*) **1** (10 mmol), ClCH₂COOH (10 mmol), AcONa (10 mmol), AcOH 5 mL, reflux, 2 h, 76%; *ii*) **3** (10 mmol), $HC(OEt)_3$ (12 mmol), Ac₂O (10 mL), reflux, 2 h, 78%; *iii*) **4** (10 mmol), appropriate amino derivatives (10 mmol), EtOH, reflux, 2 h.

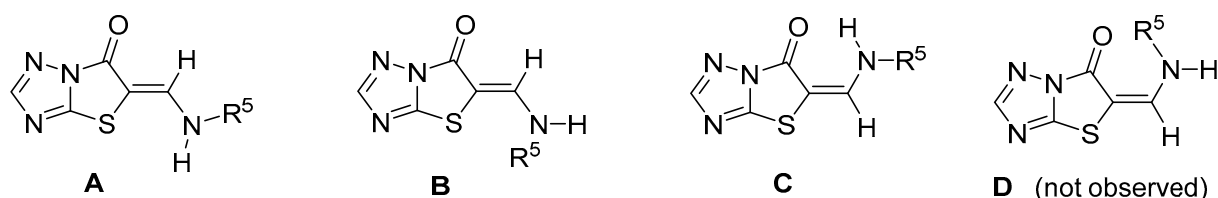
2.2. Spectral Characterization

The structures of the derivatives **2a-l**, **5a-h**, **6a-d** were confirmed by the ¹H-NMR, ¹³C-NMR, 2D NMR and LC-MS, (copies of the corresponding spectra are presented in the Supplementary Material).

The ¹H-NMR spectra of **5a-h** contained signals for protons of the double bond at 8.14–8.17 ppm for **5a-c** ($R^5 = \text{Alk}$) and 8.26–8.52 for **5d-h** ($R^5 = \text{Ar or Het}$); for NH proton at 8.78–9.06 ppm for **5a-c** (9.29–10.77 for **5d-h**); for the 1,2,4-triazole ring proton at

8.14–8.16 ppm for **5a–c** (8.30–8.40 ppm for **5d–h**) and signals of appropriate substituents. The ^{13}C -NMR spectra contained four respective signals for a bicyclic system and one signal for the ethylene moiety. The assignment in **5b**, **5c** was made based on HSQC and HMBC experiments.

Compounds **5a–h** can exist in four possible stereoisomeric forms A–D (Scheme 3) which significantly vary by stereochemistry of double bond and relative orientation of substituent R^5 .



Scheme 3. Possible stereoisomeric/rotameric forms of **5a–h**.

The ^1H -NMR spectra of pure samples **5b,d–h**, beside the signals of the main stereoisomer (I), contained minor signals with relative intensity ~5–15% which were assigned to an additional stereoisomer.

Compound **5c** ($\text{R}^5 = \text{cyclopropyl}$) provided a triple set of signals with relative intensity 62:31:7, presumably for three stereoisomers, I, II and III respectively (Figure 3). The coupling constant 3J between ethylene and NH protons (13.9 Hz) in III isomer indicates the *trans*-orientation of these protons which corresponds to either A or C isomer (Scheme 3). The assignment between A and C isomers can be performed based on chemical shifts of NH protons. The chemical shift of NH proton in III isomer is shifted downfields by 0.30 ppm as compared to the I isomer which can be explained by intramolecular interactions which are realized in the C isomer (Scheme 3). Therefore, isomers I (62%), II (31%) and III (7%) probably correspond to structures A, B, and C, respectively.

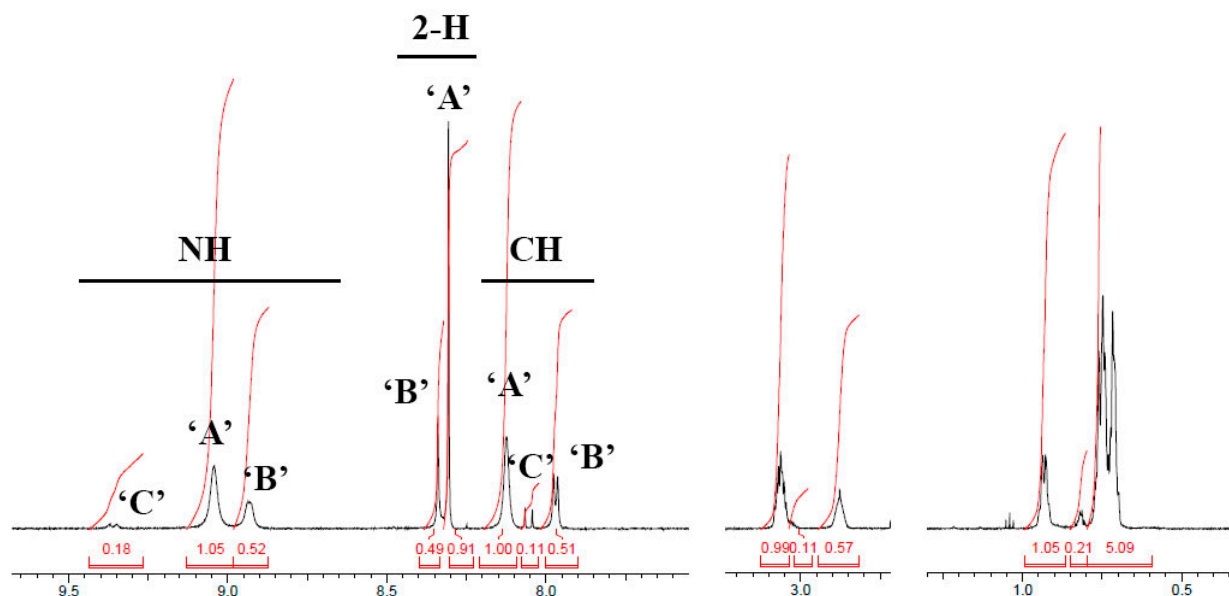


Figure 3. ^1H -NMR spectrum of **5c**. Signals of A, B, C forms of **5c** are shown.

The NOESY spectrum of **5c** (Figure 4, Supplementary Figure S1) contained EXSY peaks for ethylene, NH and aliphatic protons of I, II and III isomers which indicates the co-existence of those forms of **5c**.

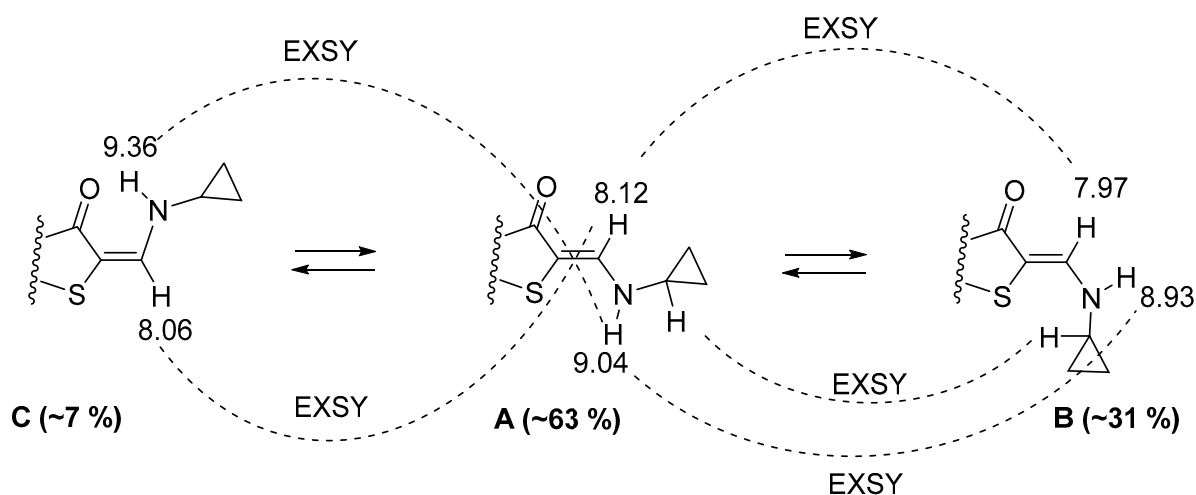
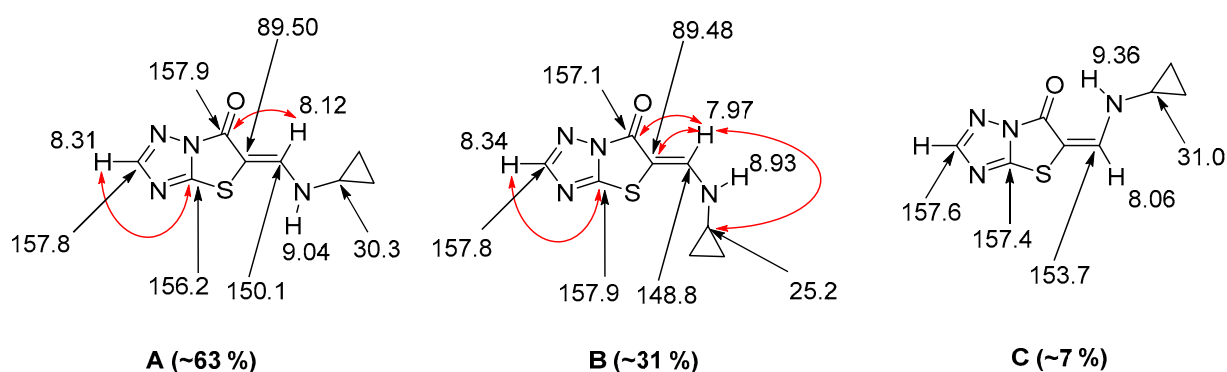


Figure 4. Interpretation of exchange cross-peaks between A, B and C isomers of 5c.

In the ^{13}C -NMR spectrum of 5c signals of A and B form and some signals of C form could be identified (Scheme 4).



Scheme 4. ^1H and ^{13}C -NMR chemical shifts of (A–C) isomers of 5c with key interactions in the relevant HMBC spectra.

The similar pattern of triplicate signals in the ^1H -NMR spectrum was observed for 5a ($\text{R}^5 = \text{CH}_3$) and showed the presence of three stereoisomeric/rotameric forms A, B, C with relative intensity 80:10:10, respectively. The coupling constants between NH and ethylene protons for A and C forms were 11.6 and 14.4 Hz, respectively, whereas for form B the 3J was 7.5 Hz which corresponding of the stereochemistry provided in Scheme 3. Only one type of signals for 5a ($\text{R}^5 = \text{CH}_3$) was observed in the ^{13}C -NMR spectrum.

The ^1H -NMR for 5b ($\text{R}^5 = \text{CH}_2\text{COOH}$) showed the presence of two isomers, A and C, with relative intensity 85:15, respectively. The coupling constants between NH and ethylene protons for A and C isomers were both 14.2 Hz, which corresponds to stereochemistry provided in Scheme 3. The NOESY spectrum has showed proximity between CH_2 and ethylene = CH protons as an additional confirmation of the stereochemistry of A and C isomer which allows excluding the B isomer for this compound. 2D NMR data for 5b showed that A and C isomers of 5b exhibited the stereochemistry similar to those for compound 5c ($\text{R}^5 = \text{cyclopropyl}$).

Taking into account the similarity in chemical shift values for A and C forms, the structure A can be proposed as the main isomer for all derivatives 5a–h, C as a minor isomer and, no B form in most cases (it appears only in 5a and 5c).

Isomer A of 5a–c showed either the presence of AX system with $^3J = 11.6 \dots 14.2$ Hz for NH proton and for the proton of the ethane moiety or two broad singlets for these protons. This can be due to the velocity of $\text{A} > \text{B}$ transformation which may be susceptible to different factors such as concentration, trace of water, etc.

To evaluate the presence of the rotamer forms we have studied the dependence of the $^1\text{H-NMR}$ spectra pattern for compound **5c** on the temperature. The tripling of the signals in the spectra of **5c** had been gradually lost at 60 °C until the signals coalesce completely at 100 °C, therefore, the complication of $^1\text{H-NMR}$ spectra is connected with hindered rotation. Compounds **2a–l**, **6a–d** showed $^1\text{H-}$ and $^{13}\text{C-NMR}$ data similar to those for **A** isomer of **5a–h**, although no traces of additional stereoisomers were found.

2.3. The X-ray Crystal Structure Analysis of (Z)-5-Cyclopropylaminomethylidene-[1,3]thiazolo[3,2-b][1,2,4]triazol-6(5H)-one (**5c**)

The molecular structure of **5c** and the atom-labelling scheme are illustrated in Figure 5. The molecule consists of the eight-membered thiazolo[3,2-b][1,2,4]triazol-6(5H)-one system and the *N*-cyclopropylaminomethylidene residue located at the C5 atom. The fused bicyclic system is approximately planar with an r.m.s. deviation of 0.0245 Å. The interatomic C5–C7 distance observed [1.373(2) Å] confirms the presence of a double bond between these atoms. The *N*-cyclopropylamino moiety is in *Z* configuration with respect to the bicyclic moiety. The torsion angle S4–C5–C7–N8 is $-0.1(3)^\circ$.

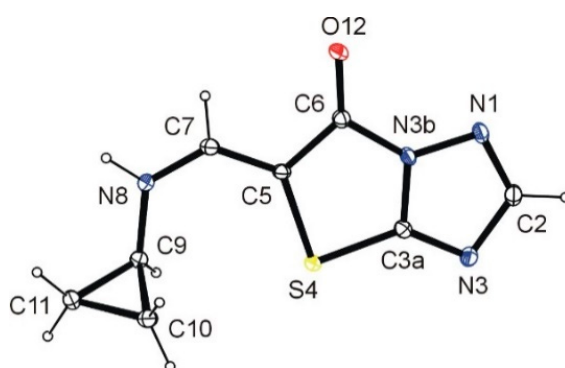


Figure 5. A view of **5c**, showing the atomic labelling scheme. Non-H atoms are drawn as 30% probability displacement ellipsoids and H atoms are drawn as spheres of an arbitrary size.

The molecules of **5c** highlight the presence of quite strong resonance effect involving the carbonyl group and the exocyclic N8 atom via the double bond C5–C7. This is indicated by the C6–O12 [1.2293(19) Å], C5–C6 [1.438(2) Å], C5–C7 [1.373(2) Å], and C7–N8 [1.320(2) Å] bonds which are all significantly distorted with respect to the typical lengths of the C=O [1.210(1) Å], Csp^2-Csp^2 [1.478(4) Å], C=C [1.331(1) Å] and Csp^2-N [1.355(3) Å] bonds [36].

In the crystal of **5c**, the molecules related by screw axis 2_1 are connected by the classical N8–H8 \cdots O12ⁱ hydrogen bonds into chains (Supplementary Figure S2a, Table 1). It is worth noting that in the chains, the molecules, or rather their planar thiazolo[3,2-b][1,2,4]triazol-6(5H)-one ring systems, are arranged coplanar to each other to form tapes with the best plane parallel to the plane (−203). The adjacent anti-parallel chains of molecules are further joined by hydrogen bonds C11–H11A \cdots N3ⁱⁱ into layers showing a stepped shape, with mean plane parallel to the plane (−102) (Supplementary Figure S2b, Table 1). There are π -electron interactions between the adjacent layers (Supplementary Figure S3). The perpendicular distances between partially overlapping thiazolo[3,2-b][1,2,4]triazol-6(5H)-one (ThiTri) systems are 3.4409 (6) Å and 3.4100 (6) Å for $\pi(\text{ThiTri})\cdots\pi(\text{ThTri})^{\text{iii}}$ and $\pi(\text{ThiTri})\cdots\pi(\text{ThTri})^{\text{iv}}$, respectively [symmetry codes: (iii) $x, 3/2 - y, 1/2 + z$, (iv) $x, 3/2 - y, -1/2 + z$].

Table 1. Hydrogen-bond geometry (Å) for **5c**.

<i>D</i> —H \cdots <i>A</i>	<i>D</i> —H	H \cdots <i>A</i>	<i>D</i> \cdots <i>A</i>	<i>D</i> —H \cdots <i>A</i>
N8—H8 \cdots O12 ⁱ	0.85 (2)	1.95 (2)	2.7844 (17)	168 (2)
C11—H11B \cdots N3 ⁱⁱ	0.99	2.61	3.603 (2)	179

Symmetry codes: ⁱ $1 - x, -1/2 + y, 1/2 - z$; ⁱⁱ $2 - x, 1 - y, 1 - z$.

2.4. In Vitro Evaluation of the Anticancer Activity and Cytotoxicity. Compare Analysis

Compounds **2a**, **2c–f**, **2h–l**, **3**, **5e**, **5f** were selected for antitumor activity which was performed according to the standard protocols of National Cancer Institute (NCI, Bethesda, MD, USA) Developmental Therapeutic Program (DTP) [37–40]. At the prescreening stage, the compounds were evaluated for antitumor activity at the concentration of 10 μ M against a panel of approximately sixty cancer cell lines representing different types of cancer including leukemia, melanoma, lung, colon, CNS, ovarian, renal, prostate and breast cancers. The results of the prescreening assay are summarized in Table 2.

Table 2. Anticancer screening data in concentration 10 μ M.

Compound	60 Cell Lines Assay in One Dose, 10 μ M				
	Mean Growth, %	Range of Growth, %	Most Sensitive Cell Line(s) (Growth Inhibition Percent)/Panel	Positive Cytostatic Effect ^a	Positive Cytotoxic Effect ^b
2a	89.98	52.79 to 122.91	NCI-H522 (52.79)/NSCLC [#]	0/59	0/59
2c	102.57	77.10 to 146.05	NCI-H522 (77.10)/NSCLC [#]	0/59	0/59
2d	99.67	−73.92 to 147.73	CCRF-CEM (−73.92), HL-60 (TB) (−58.44), MOLT-4 (−73.62) all Leukemia	2/58	3/58
2e	101.82	61.87 to 133.86	SR (61.87)/ Leukemia	0/58	0/58
2f	108.16	86.65 to 261.80	OVCAR-5 (86.65)/ Ovarian Cancer HL-60 (TB) (−32.79), MOLT-4 (−11.15), RPMI-8226 (−16.52), SR (−48.01)/all Leukemia ; HOP-92 (−21.66)/NSCLC [#] ;	0/57	0/57
2h	28.98	−48.01 to 121.70	BT-549 (−16.67), HS 578T (−15.94)/all Breast Cancer ; RXF 393 (−15.19)/ Renal Cancer ; LOX IMVI (−9.62)/ Melanoma ; DU-145 (−21.71)/ Prostate Cancer ; SF-539 (−33.43), SNB-75 (−11.46)/ CNS Cancer	30/57	12/57
2i	61.05	−22.54 to 122.94	CCRF-CEM (−3.49); SR (−25.54) all Leukemia	17/58	2/58
2j	106.32	82.41 to 135.61	K-562 (82.41)/ Leukemia	0/56	0/56
2k	110.51	25.23 to 180.21	SR (25.23)/ Leukemia	1/56	0/56
2l	105.41	66.88 to 141.12	PC-3 (66.88)/ Prostate Cancer	0/59	0/59
3	97.21	74.85 to 122.06	SR (74.85)/ Leukemia	0/59	0/59
5e	100.59	80.34 to 137.75	T-47D (80.34)/ Breast Cancer	0/59	0/59
5f	93.61	54.41 to 111.61	T-47D (54.41)/ Breast Cancer	0/59	0/59

NSCLC[#]: Non-Small Cell Lung Cancer. ^a Ratio between number of cell lines with percent growth from 0 to 50 and total number of cell lines.

^b Ratio between number of cell lines with percent growth of <0 and total number of cell lines.

Overall, the 5-ene-thiazolo[3,2-*b*][1,2,4]triazole-6(5*H*)-ones exhibited a range of potencies against the tumor cell lines tested. Among them, three compounds (**2d**, **2h**, **2i**) presented excellent cytotoxic and four derivatives (**2d**, **2h**, **2i**, **2k**) cytostatic properties in one or more cell lines when applied at a concentration of 10 μ M. It worth noting that compounds **2d**, **2h**, **2i** had been possessing cytotoxic effect against leukemia cell lines. Also, compound **2h** has demonstrated a cytotoxic effect on some lines in prostate cancer, NSCLC, breast cancer, renal cancer, melanoma, and CNS cancer subpanels. Since compounds **2h** and **2i** exhibited the highest cytotoxic and cytostatic activity, they were selected for in-depth studies at five different concentrations (0.01, 0.1, 1.0, 10.0, and 100.0 μ M) against the same NCI-60 HTCL panel of cell lines. The outcomes were calculated and presented in the form of three response parameters (GI₅₀, TGI and LC₅₀) for each cell line via growth percentage inhibition curves [41,42]. The GI₅₀ value (growth inhibitory activity) corresponds to the concentration of compound causing 50% decrease in net cell growth, the TGI value (cytostatic activity) represents the concentration of compound resulting in total growth inhibition (100% growth inhibition) and LC₅₀ value (cytotoxic activity) demonstrate the lethal dose of compound causing net 50% death of initial cells. The results calculated are provided in Supplementary Table S2 and Table 3.

Table 3. Influence of compounds **2h** and **2i** on the growth of tumor panels (GI₅₀, TGI, LC₅₀) and selectivity index (SI) values.

Panel, MG_MID	GI ₅₀ , μM		SI (GI ₅₀)		TGI, μM		SI (TGI)		LC ₅₀ , μM		SI (LC ₅₀)	
	2h	2i	2h	2i	2h	2i	2h	2i	2h	2i	2h	2i
Leukemia	1.92	11.32	1.84	0.97	6.85	51.55	1.88	0.55	26.81	99.25	1.39	0.64
Range*	1.35–2.69	2.88–18.19	-	-	3.16–14.45	9.99->100	-	-	7.58–48.97	95.49->100	-	-
NSCLC	6.98	14.13	0.51	0.78	18.22	30.03	0.71	0.94	44.01	64.55	0.84	0.97
Range*	2.29–15.48	10.23–19.49	-	-	9.99–30.90	25.70–39.81	-	-	31.62–60.25	50.11–83.17	-	-
Colon cancer	6.13	12.42	0.58	0.88	17.39	26.51	0.74	1.06	41.39	56.32	0.90	1.12
Range*	2.45–9.33	9.55–16.59	-	-	10.96–21.37	21.37–33.11	-	-	33.11–45.70	46.77–57.60	-	-
CNS Cancer	2.87	9.85	1.23	1.11	10.76	27.42	1.19	1.03	38.58	66.25	0.96	0.95
Range*	1.77–4.07	6.02–13.18	-	-	4.46–15.48	19.05–44.66	-	-	12.59–87.09	43.65->100	-	-
Melanoma	4.79	11.77	0.74	0.93	16.49	25.61	0.78	1.10	41.20	55.37	0.90	1.14
Range*	2.63–8.31	5.62–14.79	-	-	11.22–20.89	18.19–33.11	-	-	33.11–51.28	42.65–77.62	-	-
Ovarian Cancer	8.05	13.69	0.44	0.80	20.34	31.15	0.63	0.90	52.09	68.65	0.71	0.92
Range*	2.11–15.48	6.60–12.88	-	-	5.62–30.90	20.89–38.90	-	-	19.49–97.72	51.28->100	-	-
Renal Cancer	5.37	13.02	0.66	0.84	16.40	27.13	0.78	1.03	40.46	55.02	0.92	1.15
Range*	1.62–12.58	5.75–17.37	-	-	8.12–25.11	21.37–31.62	-	-	28.84–50.11	51.28–58.88	-	-
Prostate Cancer	2.67	7.6	1.33	1.44	10.34	27.11	1.25	1.04	30.77	68.15	1.21	0.93
Range*	1.54–3.80	3.98–11.22	-	-	4.46–16.21	16.21–38.01	-	-	15.84–45.70	36.30->100	-	-
Breast Cancer	4.48	9.72	0.79	1.13	15.61	30.29	0.82	0.93	46.05	73.18	0.80	0.86
Range*	<0.01–15.48	3.54–21.87	-	-	4.07–41.68	15.84–67.06	-	-	19.49->100	41.68->100	-	-
Total MG_MID	3.54	10.96	-	-	12.88	28.18	-	-	37.15	63.09	-	-

Range*—Values range inside panel, μM; GI₅₀—molar concentration of the compound that inhibits 50% net cell growth; TGI—molar concentration of the compound leading to the total inhibition; LC₅₀ molar concentration of the compound leading to 50% net cell death.

Compound **2h** inhibited each of the 49 cancer cell lines tested in the micromolar range with GI₅₀ < 10 μM and average GI₅₀, TGI and LC₅₀ values of 3.54 μM, 12.88 μM, and 37.15 μM, respectively (Table 3). The moderate selectivity of **2h** was observed for breast cancer cell line MCF7 at GI₅₀ (SI = 4.48) and TGI (SI = 3.19) levels, and for leukemia lines: SR at TGI (SI = 3.16), CCRF-CEM at TGI (SI = 4.08) and LC₅₀ (SI = 4.90) levels. In stark contrast, compound **2i** exhibited lower inhibitory activity with GI₅₀ < 10 μM against 13 cell lines with average GI₅₀, TGI, and LC₅₀ values of 10.96 μM, 28.18 μM and 63.09 μM, respectively. A moderate selectivity was observed at GI₅₀ level for leukemia line CCRF-CEM (SI = 3.81) and breast cancer cell line HS 578T (SI = 3.01).

The mean GI₅₀ values (μM) for compounds **2h** and **2i** have been compared to the same data for standard anticancer agents as the synthetic drug cisplatin and the natural compound curcumin (Figure 6). The data demonstrates that MG_MID (μM) values for **2h** are lower than those for cisplatin except in ovarian cancer subpanel and for curcumin except in the colon cancer subpanel when tested in the same experimental setup. Meanwhile, compound **2i** showed lower activity and its MG_MID (μM) values were superior only for the colon and breast cancer subpanels in comparison with cisplatin and for the prostate cancer subpanel in comparison with curcumin.

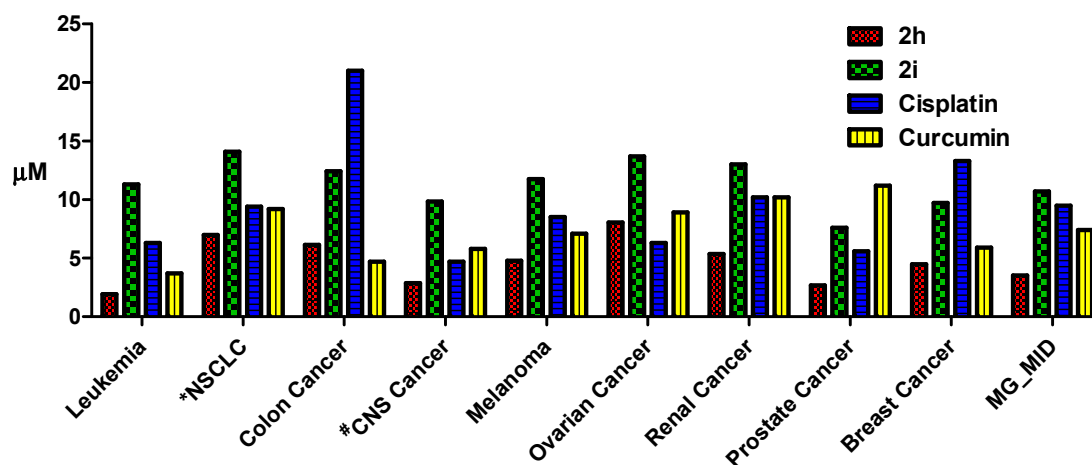


Figure 6. Mean growth inhibitory concentration (MG_MID GI₅₀, μM) of compounds **2h** and **2i** in comparison with cisplatin and curcumin. *NSCLC—Non-small Cell Lung Cancer, #CNS—Central nervous system.

The COMPARE algorithm of the NCI allows the prediction of biochemical mechanisms of action of the novel compounds on the basis of their *in vitro* activity profiles by comparing these to the ones of standard agents. The COMPARE analysis was performed for **2h** and **2i** against the NCI “Standard Agents” database at the GI₅₀ level [38–40]. The values of the Pearson correlation coefficients (PCC) higher than 0.5 were chosen as noteworthy. However, PCC values obtained did not enable the prediction of the mechanisms of cytotoxicity for the compounds tested with high probability. Both compounds showed the correlation at the GI₅₀ level only with one NCI Standard Agent—“Glyoxalic acid” (NSC:S267213, chemical name: (*E*)-2-(2-((4-methoxyphenyl)sulfonyl)hydrazono)acetic acid or glyoxylic acid *p*-methoxybenzenesulfonylhydrazono) and the PCC values were calculated as 0.561 for **2h** and 0.647 for **2i**. The alkylating mechanism of antineoplastic action has been reported for NSC:S267213 and a set of its structural analogs [43–46].

Compounds **2h** and **2i** were also evaluated *in vitro* for their cytotoxic potential against human embryonic kidney (HEK 293) cell lines using the MTT assay [47]. The IC₅₀ values obtained were 28.99 μM and 24.43 μM for **2h** and **2i**, respectively, suggest that these derivatives could effectively act against cancer cell lines without causing toxicity to normal somatic cells.

2.5. The Preliminary Structure-Anticancer Activity Relationship for Novel 5-Ene-thiazolo[3,2-*b*][1,2,4]triazole-6(5*H*)-ones

Based on the biological data obtained so far, structure-activity relationship (SAR) analysis was determined. The SAR data revealed that the anticancer activity of synthesized 5-ene-thiazolo[3,2-*b*][1,2,4]triazole-6(5*H*)-ones is dependent upon the nature of substituent connected with a double bond at C-5 of the bicyclic system. Presence of C-5 linked benzylidene moieties resulted in better activity compared to heterocyclic rings (furan (**2j**), thiophene (**2k**), *N*-AcO-indole (**2l**)). Besides it, the presence and position of a chlorine atom in the benzylidene part of molecules also plays a crucial role in the realization of the anticancer effect. So, the derivatives **2h** and **2i** with the chlorine atom and with an additional modification by *N*-(4-*R*⁴-phenyl)acetamides fragments linked at the O-2 position have been found to exert excellent antitumor activities. It is worth to note that the introduction of an imine-linker between the 4-chlorophenyl moiety and double bond at C-5 (**5f**), drastically decreased the inhibitory activity compared with data reported in [29]. Similarly, the moving of the fluorine atom from C-4 to C-2 position in benzylidene moiety (**2a**) leads to loss of activity [29]. Interestingly, that derivative containing 4-AcO-group in benzylidene core (**2d**), demonstrated inhibition of leukemia lines CCRF-CEM (−73,92), HL-60 (TB) (−58,44), MOLT-4 (−73,62) against the backdrop of the almost complete lack of impact on other cell lines. In addition, it should be noted that for all active derivatives screened at both stages, the activity against leukemia line(s) was observed which is in agreement with data described in the literature [27,29,30].

3. Materials and Methods

3.1. General Information

Melting points were measured in open capillary tubes on a BÜCHI B-545 melting point apparatus (BÜCHI Labortechnik AG, Flawil, Switzerland) and are uncorrected. The elemental analyses (C, H, N) were performed using the Perkin-Elmer 2400 CHN analyzer (PerkinElmer, Waltham, MA, USA) and were within ±0.4% of the theoretical values. The 500 MHz-¹H and 126 MHz-¹³C spectra were recorded on Bruker AVANCE-500 spectrometer and 2D spectra were recorded on a Bruker AVANCE-600 spectrometer (Bruker, Bremen, Germany). All spectra were recorded at room temperature except where indicated otherwise and were referenced internally to solvent reference frequencies. Chemical shifts (δ) are quoted in ppm and coupling constants (J) are reported in Hz. LC-MS spectra were obtained on a Finnigan MAT INCOS-50 (Thermo Finnigan LLC, San Jose, CA, USA). Solvents and reagents that are commercially available were used without further purification. The

synthetic procedure for compound **1** was described in [48], for derivatives **2a–l** in [29] and for compound **4** in [35].

3.2. Preparation and Characterization of Compounds

3.2.1. Characterization of Compounds **2a–l**

(*Z*)-5-(2-Fluorobenzylidene)thiazolo[3,2-*b*][1,2,4]triazol-6(5*H*)-one (**2a**). Yield 58%, light yellow powder, mp 192–193 °C (ethanol–DMF 4:1). ¹H-NMR (500 MHz, DMSO-*d*₆, δ): 8.53 (s, 1H, 2-H), 8.19 (s, 1H, =CH), 7.73 (t, *J* = 8.5 Hz, 1H, C₆H₄), 7.64–7.69 (m, 1H, C₆H₄), 7.46–7.49 (m, 2H, C₆H₄). ¹³C-NMR (126 MHz, DMSO-*d*₆, δ): 161.5, 159.4, 155.7, 134.3, 130.1, 129.2, 127.2, 125.5, 119.9, 116.5, 116.2. LCMS (ESI+) *m/z* 248 [M + H]⁺. Anal. calc. for C₁₁H₆FN₃O: C 53.44%, H 2.45%, N 16.99%. Found: C 53.60%, H 2.70%, N 17.20%.

(*Z*)-5-(2-Methoxybenzylidene)thiazolo[3,2-*b*][1,2,4]triazol-6(5*H*)-one (**2b**). Yield 54%, yellow powder, mp 196–198 °C (ethanol–DMF 4:1). ¹H-NMR (500 MHz, DMSO-*d*₆, δ): 8.49 (s, 1H, 2-H), 8.34 (s, 1H, =CH), 7.62–7.56 (m, 2H, C₆H₄), 7.22 (d, *J* = 8.0 Hz, 1H, C₆H₄), 7.16 (t, *J* = 7.5 Hz, 1H, C₆H₄), 3.95 (s, 3H, CH₃). ¹³C-NMR (126 MHz, DMSO-*d*₆, δ): 160.0, 159.1, 158.5, 156.5, 134.9, 134.1, 130.2, 124.7, 121.4, 120.7, 112.1, 69.1, 55.9. LCMS (ESI+) *m/z* 260 [M + H]⁺. Anal. calc. for C₁₂H₉N₃O₂S: C 55.59%, H 3.50%, N 16.21%. Found: C 55.80%, H 3.70%, N 16.40%.

(*Z*)-5-(2-(Allyloxy)benzylidene)thiazolo[3,2-*b*][1,2,4]triazol-6(5*H*)-one (**2c**). Yield 63%, brown-yellow powder, mp 133–136 °C (ethanol). ¹H-NMR (500 MHz, DMSO-*d*₆, δ): 8.50 (s, 1H, 2-H), 8.40 (s, 1H, =CH), 7.61 (d, *J* = 9.3 Hz, 1H, C₆H₄), 7.59–7.54 (m, 1H, C₆H₄), 7.23 (d, *J* = 8.5 Hz, 1H, C₆H₄), 7.17 (t, *J* = 7.3 Hz, 1H, C₆H₄), 6.12 (ddt, *J* = 15.8, 10.5, 5.2 Hz, 1H, CH₂=CH-CH₂), 5.45 (d, *J* = 1.7 Hz, 1H, CH₂=CH-CH₂), 5.34 (d, *J* = 1.6 Hz, 1H, CH₂=CH-CH₂), 4.77–4.79 (m, 2H, CH₂=CH-CH₂). ¹³C-NMR (126 MHz, DMSO-*d*₆, δ): 159.8, 159.0, 157.4, 156.3, 134.1, 133.8, 132.7, 129.7, 124.4, 121.5, 120.6, 118.1, 113.4, 68.9. LCMS (ESI+) *m/z* 286 [M + H]⁺. Anal. calc. for C₁₄H₁₁N₃O₂S: C 58.93%, H 3.89%, N 14.73%. Found: C 59.10%, H 4.00%, N 14.90%.

(*Z*)-4-((6-Oxothiazolo[3,2-*b*][1,2,4]triazol-5(6*H*)-ylidene)methyl)phenyl acetate (**2d**). Yield 53%, white-yellow powder, mp 211–213 °C (ethanol–DMF 4:1). ¹H-NMR (500 MHz, DMSO-*d*₆, δ): 8.70 (s, 1H, =CH), 8.47 (s, 1H, 2-H), 8.01 (d, *J* = 8.5 Hz, 2H, C₆H₄), 7.58 (d, *J* = 8.6 Hz, 2H, C₆H₄), 2.50 (s, 3H, CH₃). ¹³C-NMR (126 MHz, DMSO-*d*₆, δ): 169.0, 159.5, 159.2, 156.0, 152.7, 138.5, 132.0, 129.9, 124.5, 123.2, 49.7, 20.8. LCMS (ESI+) *m/z* 288 [M + H]⁺. Anal. calc. for C₁₃H₉N₃O₃S: C 54.35%, H 3.16%, N 14.63%. Found: C 54.50%, H 3.40%, N 14.80%.

(*Z*)-5-(4-(Diethylamino)benzylidene)thiazolo[3,2-*b*][1,2,4]triazol-6(5*H*)-one (**2e**). Yield 67%, light red-purple powder, mp 232–234 °C (ethanol–DMF 4:1). ¹H-NMR (500 MHz, DMSO-*d*₆, δ): 8.46 (s, 1H, 2-H), 8.10 (s, 1H, =CH), 7.60 (d, *J* = 9.1 Hz, 2H, C₆H₄), 6.86 (d, *J* = 9.1 Hz, 2H, C₆H₄), 3.47 (d, *J* = 7.1 Hz, 4H, 2*CH₂), 1.14 (t, *J* = 7.0 Hz, 6H, 2*CH₃). ¹³C-NMR (126 MHz, DMSO-*d*₆, δ): 158.8, 158.6, 156.5, 150.5, 141.1, 133.9, 118.5, 114.4, 111.9, 44.1, 12.6. LCMS (ESI+) *m/z* 301 [M + H]⁺. Anal. calc. for C₁₅H₁₆N₄O: C 59.98%, H 5.37%, N 18.65%. Found: C 60.20%, H 5.50%, N 18.80%.

(*Z*)-5-(3,4-Dimethoxybenzylidene)thiazolo[3,2-*b*][1,2,4]triazol-6(5*H*)-one (**2f**). Yield 53%, yellow powder, mp 207–209 °C (ethanol–DMF 4:1). ¹H-NMR (500 MHz, DMSO-*d*₆, δ): 8.50 (s, 1H, 2-H), 8.23 (s, 1H, =CH), 7.40 (dd, *J* = 7.4, 2.2 Hz, 1H, C₆H₃), 7.36 (d, *J* = 2.1 Hz, 1H, C₆H₃), 7.21 (d, *J* = 8.5 Hz, 1H, C₆H₃), 3.87 (s, 3H, CH₃), 3.85 (s, 3H, CH₃). ¹³C-NMR (126 MHz, DMSO-*d*₆, δ): 159.3, 159.0, 156.6, 152.4, 152.0, 149.2, 140.4, 125.2, 121.3, 114.0, 112.3, 55.8, 55.5. LCMS (ESI+) *m/z* 290 [M + H]⁺. Anal. calc. for C₁₃H₁₁N₃O₃S: C 53.97%, H 3.83%, N 14.52%. Found: C 54.10%, H 4.00%, N 14.80%.

(*Z*)-2-(4-Chloro-2-((6-oxothiazolo[3,2-*b*][1,2,4]triazol-5(6*H*)-ylidene)methyl)phenoxy)-*N*-(*m*-tolyl)acetamide (**2g**). Yield 68%, white-yellow powder, mp 260–262 °C (ethanol–DMF 4:1). ¹H-NMR (500 MHz, DMSO-*d*₆, δ): 10.18 (s, 1H, NH), 8.52 (s, 1H, 2-H), 8.40 (s, 1H, =CH), 7.64–7.58 (m, 2H, C₆H₄ + C₆H₃), 7.44 (brs, 1H, C₆H₄ + C₆H₃), 7.36 (d, *J* = 8.1 Hz, 1H, C₆H₄ + C₆H₃), 7.24–7.08 (m, 2H, C₆H₄ + C₆H₃), 6.90 (d, *J* = 7.4 Hz, 1H, C₆H₄+C₆H₃), 4.97 (s, 2H, CH₂), 2.27 (s, 3H, CH₃). ¹³C-NMR (126 MHz, DMSO-*d*₆, δ): 165.5, 159.7, 156.1, 155.9,

138.2, 138.0, 133.5, 132.8, 128.8, 128.6, 126.8, 125.4, 124.4, 122.9, 119.9, 119.9, 116.6, 115.2, 67.5, 21.2. LCMS (ESI+) m/z 428 [M + H]⁺. Anal. calc. for C₂₀H₁₅ClN₄O₃S: C 56.27%, H 3.54%, N 13.12%. Found: C 56.50%, H 3.70%, N 13.30%.

(Z)-2-(4-Chloro-2-((6-oxothiazolo[3,2-b][1,2,4]triazol-5(6H)-ylidene)methyl)phenoxy)-N-(4-chlorophenyl)acetamide (**2h**). Yield 58%, white-yellow powder, mp 224–226 °C (ethanol–DMF 4:1). ¹H-NMR (500 MHz, DMSO-*d*₆, δ): 10.39 (s, 1H, NH), 8.50 (s, 1H, 2-H), 8.39 (s, 1H, =CH), 7.70–7.54 (m, 4H, C₆H₄+C₆H₃), 7.38 (d, *J* = 8.9 Hz, 2H, C₆H₄+C₆H₃), 7.18 (d, *J* = 8.8 Hz, 1H, C₆H₄+C₆H₃), 4.99 (s, 2H, CH₂). ¹³C-NMR (126 MHz, DMSO-*d*₆, δ): 166.0, 159.7, 159.4, 156.1, 155.8, 137.4, 133.5, 132.8, 128.8, 128.7, 127.4, 126.9, 125.5, 122.9, 121.1, 115.3, 67.2. LCMS (ESI+) m/z 449 [M + H]⁺. Anal. calc. for C₁₉H₁₂Cl₂N₄O₃S: C 51.02%, H 2.70%, N 12.53%. Found: C 51.20%, H 2.90%, N 12.70%.

Ethyl(Z)-4-(3-(4-chloro-2-((6-oxothiazolo[3,2-b][1,2,4]triazol-5(6H)-ylidene)methyl)phenyl)propanamido)benzoate (**2i**). Yield 52%, white-yellow powder, mp 176–178 °C (ethanol–DMF 4:1). ¹H-NMR (500 MHz, DMSO-*d*₆, δ): 10.60 (s, 1H, NH), 8.51 (s, 1H, 2-H), 8.39 (s, 1H, =CH), 7.93 (d, *J* = 8.9 Hz, 2H, C₆H₄+C₆H₃), 7.74 (d, *J* = 8.8 Hz, 2H, C₆H₄+C₆H₃), 7.57–7.64 (m, 2H, C₆H₄+C₆H₃), 7.20 (d, *J* = 8.7 Hz, 1H, C₆H₄+C₆H₃), 5.04 (s, 2H, CH₂), 4.28 (q, *J* = 7.1 Hz, 2H, CH₂), 1.30 (t, *J* = 7.1 Hz, 3H, CH₃). ¹³C-NMR (126 MHz, DMSO-*d*₆, δ): 172.0, 166.3, 165.4, 159.7, 159.4, 156.1, 155.8, 142.6, 133.6, 132.5, 130.4, 128.8, 126.8, 125.5, 124.6, 122.9, 118.8, 115.1, 67.5, 60.6, 21.1, 14.4. LCMS (ESI+) m/z 486 [M + H]⁺. Anal. calc. for C₂₂H₁₇ClN₄O₅S: C 54.49%, H 3.53%, N 11.55%. Found: C 54.70%, H 3.80%, N 11.70%.

(Z)-5-(Furan-2-ylmethylene)thiazolo[3,2-b][1,2,4]triazol-6(5H)-one (**2j**). Yield 61%, brown-yellow powder, mp 230–232 °C (ethanol–DMF 4:1). ¹H-NMR (500 MHz, DMSO-*d*₆, δ): 8.47 (s, 1H, 2-H), 8.22 (d, *J* = 2.3 Hz, 1H, furan), 8.13 (s, 1H, =CH), 7.35 (d, *J* = 4.0 Hz, 1H, furan), 6.86 (dd, *J* = 3.6, 1.8 Hz, 1H). ¹³C-NMR (126 MHz, DMSO-*d*₆, δ): 160.1, 159.2, 156.3, 149.3, 148.8, 125.7, 122.0, 120.8, 114.1. LCMS (ESI+) m/z 220 [M + H]⁺. Anal. calc. for C₉H₅N₃O₂S: C 49.31%, H 2.30%, N 19.17%. Found: C 49.50%, H 2.50%, N 19.30%.

(Z)-5-(Thiophen-2-ylmethylene)thiazolo[3,2-b][1,2,4]triazol-6(5H)-one (**2k**). Yield 64%, brown powder, mp > 250 °C (ethanol–DMF 4:1). ¹H-NMR (500 MHz, DMSO-*d*₆, δ): 8.57 (s, 1H, =CH), 8.50 (s, 1H, 2-H), 8.19 (d, *J* = 7.0 Hz, 1H, thiophen), 7.90 (d, *J* = 3.1 Hz, 1H, thiophen), 7.39 (dd, *J* = 3.7 Hz, 1H, thiophen). ¹³C-NMR (126 MHz, DMSO-*d*₆, δ): 159.3, 156.2, 137.1, 136.7, 136.2, 135.3, 135.2, 132.7, 129.6. LCMS (ESI+) m/z 236 [M + H]⁺. Anal. calc. for C₉H₅N₃OS₂: C 45.94%, H 2.14%, N 17.86%. Found: C 46.10%, H 2.30%, N 18.00%.

(Z)-5-((1-Acetyl-1H-indol-3-yl)methylene)thiazolo[3,2-b][1,2,4]triazol-6(5H)-one (**2l**). Yield 66%, dark-yellow powder, mp > 250 °C (ethanol–DMF 4:1). ¹H-NMR (500 MHz, DMSO-*d*₆, δ): 8.37–8.43 (m, 3H, 2-H, =CH, indole), 8.15 (brs, 1H, indole), 7.91–8.11 (m, 1H, indole), 7.38–7.45 (m, 2H, indole), 2.82 (s, 3H, CH₃). ¹³C-NMR (126 MHz, DMSO-*d*₆, δ): 170.4, 166.4, 160.5, 159.2, 156.6, 135.5, 130.6, 130.0, 126.9, 125.1, 124.4, 119.5, 116.7, 114.6, 23.4. LCMS (ESI+) m/z 311 [M + H]⁺. Anal. calc. for C₁₅H₁₀N₄O₂S: C 58.06; H 3.25; N 18.05%. Found: C 58.30%, H 3.50%, N 18.20%.

3.2.2. Synthesis of 2-((1H-1,2,4-Triazol-3-yl)thio)acetic Acid (**3**)

A mixture of compound **1** (10 mmol) with the chloroacetic acid (10 mmol) and anhydrous sodium acetate was refluxed for 2 h in glacial acetic acid (10 mL). The white solid obtained was filtered, washed with ethanol and recrystallized from glacial acetic acid. Yield 76%, white powder, mp 132–134 °C (acetic acid). ¹H-NMR (500 MHz, DMSO-*d*₆, δ): 13.99 (brs, NH), 12.80 (brs, COOH), 8.47 (brs, 2-H), 3.91 (2H, s, CH₂). ¹³C-NMR (126 MHz, DMSO-*d*₆, δ): 170.0, 158.1, 144.8, 33.7. LCMS (ESI+) m/z 160 [M + H]⁺. Anal. calc. for C₄H₅N₃O₂S: C 30.19; H 3.17; N 26.40. Found: C 30.30%, H 3.40%, N 26.60%.

3.2.3. Synthesis and Characterization of Compounds **5a–h**, **6a–d**

A mixture of compound **4** (10 mmol) with the appropriate amine (10 mmol) was refluxed for 2 h in ethanol. The solid products obtained were filtered, washed with ethanol and recrystallized from ethanol or the mixture of ethanol–dimethylformamide (4:1).

(*E/Z*)-5-((Methylamino)methylene)thiazolo[3,2-*b*][1,2,4]triazol-6(5*H*)-one (**5a**). Yield 53%, bright red-purple powder, mp 239–241 °C (ethanol–DMF 4:1). A form (~80%), ¹H-NMR (500 MHz, DMSO-*d*₆, δ): 8.76 (br s, 1H, NH), 8.29 (s, 1H, 2-H), 8.16 (d, ³*J* = 11.6 Hz, 1H, =CH), 3.09 (3H, s, CH₃). B form (~10%), ¹H-NMR (500 MHz, DMSO-*d*₆, δ): 8.69 (brs, 1H, NH), 8.30 (s, 1H, 2-H), 8.05 (d, ³*J* = 7.5 Hz, 1H, =CH), 3.10 (s, 3H, CH₃). C form (~10%), ¹H-NMR (500 MHz, DMSO-*d*₆, δ): 9.12–9.24 (m, 1H, NH), 8.33 (s, 1H, 2-H), 7.95 (d, ³*J* = 14.4 Hz, 1H, =CH), 3.11 (s, 3H, CH₃). ¹³C-NMR (126 MHz, DMSO-*d*₆, δ): 157.7, 156.2, 155.9, 151.6, 88.5, 35.2. LCMS (ESI+) *m/z* 183 [M + H]⁺. Anal. calc. for C₆H₆N₄OS: C 39.55%, H 3.32%, N 30.75%. Found: C 39.70%, H 3.50%, N 30.90%.

(*E/Z*)-((6-Oxothiazolo[3,2-*b*][1,2,4]triazol-5(6*H*)-ylidene)methyl)glycine (**5b**). Yield 62%, yellow powder, mp 229 (with decomp.) °C (ethanol–DMF 4:1). A form (~85%), ¹H-NMR (500 MHz, DMSO-*d*₆, δ): 13.07 (brs, 1H, COOH), 8.95–9.08 (m, 1H, NH), 8.32 (s, 1H, 2-H), 8.17 (d, ³*J* = 14.2 Hz, 1H, =CH), 4.19 (d, ³*J* = 5.6 Hz, 2H, CH₂). ¹³C-NMR (126 MHz, DMSO-*d*₆, δ): 170.9 (COOH), 157.9 (C-2), 156.5 (C-6), 156.4 (C-3a), 151.6 (=CH), 89.95 (C-5), 49.0 (CH₂). NOESY: 8.17–9.03 (=CH ... HN), 4.19–8.17 (CH₂ ... =CH), 4.19–9.03 (CH₂ ... NH). C form, (~15%), ¹H-NMR (500 MHz, DMSO-*d*₆, δ): 13.07 (brs, 1H, OH), 9.22–9.29 (m, 1H, NH), 8.33 (s, 1H, 2-H), 7.91 (d, ³*J* = 14.2 Hz, 1H, =CH), 4.16 (d, ³*J* = 6.3 Hz, 2H, CH₂). ¹³C-NMR (126 MHz, DMSO-*d*₆, δ): 170.7 (COOH), 157.7 (C-2), 157.4 (C-3a), 156.1 (C-6), 154.9 (=CH), 88.9 (C-5), 49.7 (CH₂). NOESY: 9.26–7.91 (weak, NH ... HC=), 9.26–4.16 (NH ... H₂C), 4.16–7.91 (CH₂ ... HC=). EXSY: 9.02–9.25. LCMS (ESI+) *m/z* 227 [M + H]⁺. Anal. calc. for C₇H₆N₄O₃S: C 37.17%, H 2.67%, N 24.77%. Found: C 37.40%, H 2.90%, N 24.90%.

(*E/Z*)-5-((Cyclopropylamino)methylene)thiazolo[3,2-*b*][1,2,4]triazol-6(5*H*)-one (**5c**). Yield 54%, beige powder, mp 199–201 °C (ethanol–DMF 4:1). A form (~62%), ¹H-NMR (500 MHz, DMSO-*d*₆, δ): 9.04 (brs, 1H, NH), 8.31 (s, 1H, 2-H), 8.12 (brs, 1H, =CH), 3.04–3.10 (m, 1H, cyclopropyl), 0.87–0.98 (m, 1H, cyclopropyl), 0.66–0.80 (m, 3H, cyclopropyl). ¹³C-NMR (126 MHz, DMSO-*d*₆, δ): 157.9 (C-6), 157.8 (C-2), 156.2 (C-3a), 150.1 (=CH), 89.51 (C-5), 30.3 (cyclopropyl), 6.0 (cyclopropyl). NOESY: 8.14–9.05 (=CH ... HN), 3.07–9.05 (NH ... HC<), 3.07–8.14 (=CH ... HC<), 0.72–9.05, 0.72–8.14, 0.72–3.07, 0.72–0.95. B form (~31%), ¹H-NMR (500 MHz, DMSO-*d*₆, δ): 8.88–8.98 (m, 1H, NH), 8.35 (s, 1H, 2-H), 7.97 (d, ³*J* = 7.3 Hz, 1H, =CH), 2.84–2.93 (m, 1H, cyclopropyl), 0.66–0.80 (m, 4H, cyclopropyl). ¹³C-NMR (126 MHz, DMSO-*d*₆, δ): 157.9 (C-3a), 157.8 (C-2), 157.1 (C-6), 148.8 (=CH), 89.48 (C-5), 25.2 (cyclopropyl), 8.84 (cyclopropyl). C form (~7%), ¹H-NMR (500 MHz, DMSO-*d*₆, δ): 9.33–9.39 (m, 1H, NH), 8.06 (d, ³*J* = 13.9 Hz, 1H, =CH), 3.01–3.04 (m, 1H, cyclopropyl), 0.80–0.85 (m, 2H, cyclopropyl), 0.66–0.80 (m, 2H, cyclopropyl). ¹³C-NMR (126 MHz, DMSO-*d*₆, δ): 157.6 (C-3a), 157.4 (C-2), 153.7 (C-6), 31.0 (cyclopropyl), 6.2 (cyclopropyl). EXSY: 9.36–8.93 (C-B), 9.36–9.06 (C-A), 8.93–9.06 (B-A), 8.06–7.97 (C-B), 8.14–8.06 (A-C), 7.97–8.14 (B-A), 2.87–3.07 (B-A). LCMS (ESI+) *m/z* 209 [M + H]⁺. Anal. calc. for C₈H₈N₄OS: C 46.14%, H 3.87%, N 26.90%. Found: C 46.30%, H 4.00%, N 27.10%.

(*E/Z*)-5-((Phenylamino)methylene)thiazolo[3,2-*b*][1,2,4]triazol-6(5*H*)-one (**5d**). Yield 56%, brown-yellow powder, mp 262–263 °C (ethanol–DMF 4:1). A form (~90%), ¹H-NMR (500 MHz, DMSO-*d*₆, δ): 10.76 (brs, 1H, NH), 8.52 (brs, 1H, =CH), 8.38 (s, 1H, 2-H), 7.37–7.42 (m, 4H, C₆H₅), 7.13–7.17 (m, 1H, C₆H₅). ¹³C-NMR (126 MHz, DMSO-*d*₆, δ): 158.3, 156.9, 156.8, 155.5, 141.8, 129.7, 124.5, 117.1, 94.7. C form (~10%), ¹H-NMR (500 MHz, DMSO-*d*₆, δ): 10.72 (brs, 1H, NH), 8.68 (d, ³*J* = 13.6 Hz, 1H, =CH), 8.39 (s, 1H, 2-H), 7.37–7.42 (m, 4H, C₆H₅), 7.13–7.17 (m, 1H, C₆H₅). LCMS (ESI+) *m/z* 245 [M + H]⁺. Anal. calc. for C₁₁H₈N₄OS: C 54.09%, H 3.30%, N 22.94%. Found: C 54.20%, H 3.50%, N 23.10%.

(*E/Z*)-5-(((3-Hydroxyphenyl)amino)methylene)thiazolo[3,2-*b*][1,2,4]triazol-6(5*H*)-one (**5e**). Yield 55%, brown-yellow powder, mp 269–271 °C (ethanol–DMF 4:1). A form (~90%), ¹H-NMR (500 MHz, DMSO-*d*₆, δ): 10.68 (brs, 1H, NH), 9.69 (s, 1H, OH), 8.40 (brs, 1H, =CH), 8.38 (s, 1H, 2-H), 7.13–7.23 (m, 1H, C₆H₄), 6.78–6.85 (m, 1H, C₆H₄), 6.69–6.78 (m, 1H, C₆H₄), 6.52–6.62 (m, 1H, C₆H₄). ¹³C-NMR (126 MHz, DMSO-*d*₆, δ): 158.5, 158.3, 157.0, 156.8, 141.5, 140.9, 130.6, 111.8, 107.6, 104.2, 94.5. C form (~10%), ¹H-NMR (500 MHz, DMSO-*d*₆, δ): 10.61 (brs, 1H, NH), 9.73 (s, 1H, OH), 8.63 (d, ³*J* = 12.6 Hz, 1H, =CH), 8.38 (s, 1H, 2-H),

6.84–6.88 (m, 2H, C₆H₄), 6.57–6.61 (m, 2H, C₆H₄). LCMS (ESI+) *m/z* 261 [M + H]⁺. Anal. calc. for C₁₁H₈N₄O₂S: C 50.76%, H 3.10%, N 21.53%. Found: C 50.90%, H 3.40%, N 21.70%.

(*E/Z*)-5-(((4-Chlorophenyl)amino)methylene)thiazolo[3,2-*b*][1,2,4]triazol-6(5*H*)-one (**5f**). Yield 64%, yellow powder, mp > 280 °C (ethanol–DMF 4:1). A form (~90%), ¹H-NMR (500 MHz, DMSO-*d*₆, δ): 10.77 (1H, s, NH), 8.51 (brs, 1H, =CH), 8.40 (s, 1H, 2-H), 7.39–7.45 (m, 4H, C₆H₄). ¹³C-NMR (126 MHz, DMSO-*d*₆, δ): 158.3, 157.0, 156.7, 155.6, 141.6, 129.5, 128.2, 118.9, 95.6. C form (~10%), ¹H-NMR (500 MHz, DMSO-*d*₆, δ): 10.74 (brs, 1H, NH), 8.62 (d, ³*J* = 13.2 Hz, 1H, =CH), 8.40 (s, 1H, 2-H), 7.49–7.52 (m, 2H, C₆H₄), 7.45–7.48 (m, 2H, C₆H₄). LCMS (ESI+) *m/z* 280 [M + H]⁺. Anal. calc. for C₁₁H₇ClN₄OS: C 47.40%, H 2.53%, N 20.10%. Found: C 47.60%, H 2.70%, N 20.30%.

(*E/Z*)-5-(((Furan-2-ylmethyl)amino)methylene)thiazolo[3,2-*b*][1,2,4]triazol-6(5*H*)-one (**5g**). Yield 71%, light pink powder, mp 176–178 °C (ethanol). A form (~90%), ¹H-NMR (500 MHz, DMSO-*d*₆, δ): 9.29 (s, 1H, NH), 8.30 (s, 1H, 2-H), 8.26 (brs, 1H, =CH), 7.66–7.69 (m, 1H, furan), 6.44–6.46 (m, 1H, furan), 6.41–6.44 (m, 1H, furan), 4.62 (s, 2H, CH₂). ¹³C-NMR (126 MHz, DMSO-*d*₆, δ): 157.9, 156.5, 156.3, 150.6, 150.3, 143.3, 110.7, 108.6, 89.8, 44.7. C form (~10%), ¹H-NMR (500 MHz, DMSO-*d*₆, δ): 9.43–9.50 (m, 1H, NH), 8.31 (s, 1H, 2-H), 8.06 (d, ³*J* = 13.9, 1H, =CH), 7.65–7.66 (m, 1H, furan), 6.39–6.41 (m, 1H, furan), 4.58 (d, ³*J* = 4.73, 2H, CH₂). LCMS (ESI+) *m/z* 249 [M + H]⁺. Anal. calc. for C₁₀H₈N₄O₂S: C 48.38%, H 3.25%, N 22.57%. Found: C 48.50%, H 3.40%, N 22.80%.

(*E/Z*)-5-(((5-Methylisoxazol-3-yl)amino)methylene)thiazolo[3,2-*b*][1,2,4]triazol-6(5*H*)-one (**5h**). Yield 54%, yellow powder, mp 243–245 °C (ethanol–DMF 4:1). A form (~95%) ¹H-NMR (500 MHz, DMSO-*d*₆, δ): 11.32 (brs, 1H, NH), 8.40 (s, 1H, 2-H), 8.32 (brs, 1H, =CH), 6.41 (s, 1H, isoxazol), 2.39 (s, 3H, CH₃). ¹³C-NMR (126 MHz, DMSO-*d*₆, δ): 171.2, 159.9, 158.7, 157.7, 156.8, 140.5, 98.5, 94.2, 12.3. C form (~5%) ¹H-NMR (500 MHz, DMSO-*d*₆, δ): 10.79 (d, ³*J* = 13.2 Hz, 1H, NH), 8.46 (d, ³*J* = 13.2 Hz, 1H, =CH). LCMS (ESI+) *m/z* 250 [M + H]⁺. Anal. calc. for C₉H₇N₅O₂S: C 43.37%, H 2.83%, N 28.10%. Found: C 43.50%, H 3.00%, N 28.30%.

(*Z*)-5-(Indolin-1-ylmethylene)thiazolo[3,2-*b*][1,2,4]triazol-6(5*H*)-one (**6a**). Yield 57%, yellow-brown powder, mp > 250 °C (ethanol–DMF 4:1). ¹H-NMR (500 MHz, DMSO-*d*₆, δ): 8.62 (s, 1H, =CH), 8.43 (s, 1H, 2-H), 7.58 (d, *J* = 8.1 Hz, 1H, C₆H₄), 7.36 (d, *J* = 7.3 Hz, 1H, C₆H₄), 7.29 (t, *J* = 7.7 Hz, 1H, C₆H₄), 7.14 (t, *J* = 7.3 Hz, 1H, C₆H₄), 4.42 (t, *J* = 8.0 Hz, 2H, CH₂), 3.37 (t, *J* = 8.0 Hz, 2H, CH₂). ¹³C-NMR (126 MHz, DMSO-*d*₆, δ): 158.3, 157.8, 156.7, 142.3, 138.9, 131.5, 128.1, 126.1, 125.0, 111.0, 93.1, 49.2, 27.7. LCMS (ESI+) *m/z* 271 [M + H]⁺. Anal. calc. for C₁₃H₁₀N₄OS: C 57.76%, H 3.73%, N 20.73%. Found: C 57.90%, H 3.90%, N 20.90%.

(*Z*)-5-(Piperidin-1-ylmethylene)thiazolo[3,2-*b*][1,2,4]triazol-6(5*H*)-one (**6b**). Yield 61%, beige powder, mp 190–192 °C (ethanol). ¹H-NMR (500 MHz, DMSO-*d*₆, δ): 8.35 (s, 1H, 2-H), 8.12 (s, 1H, =CH), 3.64 (s, 4H, piperidine), 1.65 (s, 6H, piperidine). ¹³C-NMR (126 MHz, DMSO-*d*₆, δ): 157.8, 157.1, 156.7, 149.1, 148.7, 96.8, 86.2, 22.9. LCMS (ESI+) *m/z* 237 [M + H]⁺. Anal. calc. for C₁₀H₁₂N₄OS: C 50.83%, H 5.12%, N 23.71%. Found: C 51.10%, H 5.40%, N 23.90%.

(*Z*)-5-((4-(2-Hydroxyethyl)piperazin-1-yl)methylene)thiazolo[3,2-*b*][1,2,4]triazol-6(5*H*)-one (**6c**). Yield 67%, light pink powder, mp 189–192 °C (ethanol). ¹H-NMR (500 MHz, DMSO-*d*₆, δ): 8.35 (s, 1H, 2-H), 8.13 (s, 1H, =CH), 4.47 (t, *J* = 5.3 Hz, 1H, OH), 3.65 (d, *J* = 5.6 Hz, 4H, piperazine), 3.52 (q, *J* = 6.0 Hz, 2H, CH₂), 2.58 (dd, *J* = 6.1, 4.2 Hz, 4H, piperazine), 2.45 (t, *J* = 6.1 Hz, 2H, CH₂). ¹³C-NMR (126 MHz, DMSO-*d*₆, δ): 157.9, 157.0, 156.0, 155.8, 148.9, 86.8, 59.7, 59.2, 58.4. LCMS (ESI+) *m/z* 282 [M + H]⁺. Anal. calc. for C₁₁H₁₅N₅O₂S: C 46.96%, H 5.37%, N 24.89%. Found: C 47.10%, H 5.60%, N 25.00%.

Ethyl(*Z*)-4-((6-oxothiazolo[3,2-*b*][1,2,4]triazol-5(6*H*)-ylidene)methyl)piperazine-1-carboxylate (**6d**). Yield 62%, beige powder, mp 204–206 °C (ethanol–DMF 4:1). ¹H-NMR (500 MHz, DMSO-*d*₆, δ): 8.37 (s, 1H, 2-H), 8.19 (s, 1H, =CH), 4.07 (q, *J* = 7.1 Hz, 2H, CH₂), 3.69 (brs, 4H, piperazine), 3.55 (brs, 4H, piperazine), 1.20 (t, *J* = 7.1 Hz, 3H, CH₃). ¹³C-NMR (126 MHz, DMSO-*d*₆, δ): 158.1, 157.3, 156.2, 154.5, 149.2, 111.6, 87.5, 61.2, 14.5. LCMS (ESI+) *m/z* 310

[M + H]⁺. Anal. calc. for C₁₂H₁₅N₅O₃S: C 46.59%, H 4.89%, N 22.64%. Found: C 46.90%, H 5.00%, N 22.80%.

3.3. Crystal Structure Determination of (E/Z)-5-((Cyclopropylamino)methylenethiazolo-[3,2-b]-[1,2,4]-triazol-6(5H)-one (5c)

3.3.1. Crystal Data

C₈H₈N₄OS, Mr = 208.24, monoclinic, space group P2₁/c, a = 9.8291(4), b = 12.1556(4), c = 7.4814(3) Å, β = 95.025(4)°, V = 890.44(6) Å³, Z = 4, D_{calc} = 1.553 g/cm³, μ = 3.005 mm⁻¹, T = 130.0(1) K.

3.3.2. Data Collection

A yellow lath crystal (MeOH) of 0.24 × 0.13 × 0.03 mm was used to record 9342 (Cu Kα-radiation, θ_{max} = 76.52°) intensities on a SuperNova Dual Atlas diffractometer (Rigaku, Oxford, UK) [49] using mirror monochromatized Cu Kα radiation from a high-flux microfocus source (λ = 1.54178 Å). Accurate unit cell parameters were determined by least-squares techniques from the θ values of 3457 reflections, θ range 4.48–76.30°. The data were corrected for Lorentz polarization and for absorption effects [49]. The 1850 total reflections (R_{int} = 0.034) were used for structure determination.

3.3.3. Structure Solution and Refinement

The structure was solved by dual-space algorithm (SHELXT) [50], and refined against F² for all data (SHELXL-97) [51]. The positions of the H atom bonded to N atom were obtained from the difference Fourier map and were refined freely. The remaining H atoms were placed geometrically in calculated positions and were refined with a riding model, with C–H = 0.99 Å (CH₂), 1.00 Å (Csp³H), 0.95 Å (Csp²H) and U_{iso}(H) = 1.2U_{eq}(C). Final refinement converged with R = 0.0305 (for 1639 data with F² > 4σ(F²)), wR = 0.0836 (on F² for all data), and S = 1.105 (on F² for all data). The largest difference peak and hole was 0.322 and −0.250 eÅ³. The molecular illustrations were drawn using ORTEP-3 for Windows [52]. Software used to prepare material for publication was WINGX [52], OLEX [53] and PLATON [54].

The supplementary crystallographic data of 5c have been deposited at the Cambridge Crystallography Data Centre (CCDC) as supplementary publication CCDC2046355. Copies of the data can be obtained, free of charge, on application to CCDC, 12 Union Road, Cambridge CB2 1EZ, UK, (Fax: +44-(0)1223-336033 or e-mail: deposit@ccdc.cam.ac.uk).

3.4. Anticancer Activity Screening (NCI-60 Human Tumor Cell Lines Screen)

The primary anticancer assay was performed on a panel of approximately sixty human tumor cell lines derived from nine neoplastic diseases (leukemia, melanoma, lung, colon, CNS, ovarian, renal, prostate, and breast cancers), in accordance with the protocol of the National Cancer Institute Drug Evaluation Branch (Bethesda, MD, USA) [37–40]. Tested compounds were added to the culture at a single concentration (10⁻⁵ M) and the cultures were incubated for 48 h. End-point determinations were made with a protein-binding dye, sulforhodamine B (SRB). Results for each tested compound were reported as the percentage of the growth of the treated cells when compared to the untreated control cells. The percentage of the growth was evaluated spectrophotometrically versus controls not treated with test agents. The cytotoxic and/or growth inhibitory effects of the most active selected compounds were tested in vitro against the full panel of human tumor cell lines at concentrations ranging from 10⁻⁴ to 10⁻⁸ M. 48-h continuous drug exposure protocol was followed and an SRB protein assay was used to estimate cell viability or growth. Using absorbance measurements [time zero (Tz), control growth in the absence of drug (C), and test growth in the presence of the drug (Ti)], the percentage growth was calculated for each drug concentration. Percentage growth inhibition was calculated as:

$$[(Ti - Tz)/(C - z)] \times 100 \quad (1)$$

for concentrations for which $T_i \geq T_z$, $[(T_i - T_z)/T_z] \times 100$ for concentrations for which $T_i < T_z$. Dose-response parameters (GI_{50} , TGI) were calculated for each compound. Growth inhibition of 50% (GI_{50}) was calculated from $[(T_i - T_z)/(C - T_z)] \times 100 = 50$, which is the drug concentration resulting in a 50% lower net protein increase in the treated cells (measured by SRB staining) as compared to the net protein increase seen in the control cells. The drug concentration resulting in total growth inhibition (TGI) was calculated from $T_i = T_z$. Values were calculated for each of these parameters if the level of activity was reached; however, if the effect was not reached or was excessive, the value for that parameter was expressed as more or less than the maximum or minimum concentration tested. The lowest values were obtained with the most sensitive cell lines. Compounds having GI_{50} values $\leq 100 \mu\text{M}$ were declared to be active. The selectivity index (SI) calculated by dividing the full panel MG_MID (full-panel mean-graph midpoint) (μM) of the compounds **2h** and **2i** by their individual subpanel MG_MID of a cell line (μM) was considered as a measure of compounds' selectivity. Ratios between 3 and 6 mean moderate selectivity, ratios greater than 6 indicate high selectivity toward the corresponding cell line, while compounds not meeting either of these criteria are rated nonselective [38,55].

3.5. Cytotoxicity Study

The cytotoxicity of compounds **2h** and **2i** was analyzed in vitro by the MTT colorimetric assay on human embryonic kidney cell lines (HEK 293) [47]. HEK cell lines were cultured in DMEM supplemented with 10% fetal calf serum and 1% antibiotic-antimycotic mixture culture plates at 37 °C and 5% CO₂-humidified incubator. Cells were seeded at a density of 1×10^5 cells/well in 96-well plate for 24 h; then, cells were washed and incubated in fresh medium. Compounds **2h** and **2i** were added at a concentration of 1, 5, 10, 25, and 50 $\mu\text{g}/\text{mL}$ to triplicate wells and kept for 24 h, after which cells were washed three times with PBS. After washing, 20 μL of MTT solution (5 mg/mL stock solution) were added to each well, and cells were then incubated for an additional 4 h. The unreacted MTT dye and medium were aspirated off, and 100 μL of DMSO was added to each well to ensure solubilization of formazan crystals. The contents of the plates were mixed for 15 min to achieve complete solubilization of the formazan crystals, and the measurement of optical density was carried out at 570 nm with a micro plate spectrophotometer (MRX Microplate Reader, Dynatech Laboratories Inc., Chantilly, VA, USA) at 570 nm.

4. Conclusions

The synthesis of a series of novel 5-aryl(heteryl)idene- and 5-aminomethylidene derivatives of thiazolo[3,2-*b*][1,2,4]triazole-6(5*H*)-one has been achieved and the synthetic pathway for 5-aminomethylidene-thiazolo[3,2-*b*][1,2,4]triazole-6(5*H*)-ones confirmed using X-ray analysis. The stereochemistry and *E/Z*-isomerization of 5-aminomethylidene-thiazolo[3,2-*b*][1,2,4]triazole-6(5*H*)-ones have been studied using ¹H-, ¹³C- and 2D NMR spectral analysis. The derivatives synthesized have been evaluated for their anticancer activity and it has been possible to identify several hits with anticancer properties and low cytotoxicity to the mammalian cells which should be study further as part of more detailed investigations into this special and especially promising class of heterocyclic compounds. The obtained data contributes to the SAR profile of 5-ene-thiazolo[3,2-*b*][1,2,4]triazole-6(5*H*)-ones for further exploration to design improved and optimized molecules with antitumor activity.

Supplementary Materials: The following are available online. Table S1: NCI numbers of compounds selected for screening. Table S2: Influence of compounds **2h** and **2i** on the growth of tumor panels, Figures S1–S49: Copies of ¹H-, ¹³C-NMR spectra of compounds **2a**, **2c**, **2d**, **2h**, **2i**, **2l**, **3**, **5a–h**, **6b**, **6c**; 2D NMR and LC-MS spectra of compounds **5b,c**.

Author Contributions: Conceptualization, S.H. and R.L.; methodology, S.H. and R.L.; software, A.G.; validation, S.H., S.K. and A.C.; formal analysis, S.H., A.G. and A.C.; investigation, S.H., S.K., S.S., A.C. and A.G.; writing—original draft preparation, S.H., S.K., A.G., A.C. and R.L.; writing—review

and editing—S.H., A.G., A.C. and R.L.; supervision, R.L.; project administration, R.L. All authors have read and agreed to the published version of the manuscript.

Funding: This research was supported by Ministry of Healthcare of Ukraine (0121U100690).

Institutional Review Board Statement: Not applicable.

Informed Consent Statement: Not applicable.

Data Availability Statement: The data presented in this study are available in this article.

Acknowledgments: Authors are grateful to G. Morris (Drug Synthesis and Chemistry Branch, National Cancer Institute, Bethesda, MD, USA), for in vitro evaluation of anticancer activity; A. Luzhetskyy, A. Paluszczak, M. Stierhof (Department of Pharmaceutical Biotechnology, Saarland University, Germany), V. Chebanov, V. Musatov (STC “Institute for Single Crystals” NAS of Ukraine), N. Trotsko (Department of Organic Chemistry, Medical University of Lublin) for LC-MS, NMR spectra and cytotoxicity studies. This paper is dedicated to the memory of our two colleagues that recently passed away. Sergiy Komykhov, who is a co-author of this paper passed away when the paper was in the final stage of preparation for submission. His contribution to this work as well as help and valuable suggestions in the past are highly appreciated. Sergiy Komykhov will be remembered as an outstanding scientist, bright mind, and good friend that loved what he was doing and shared his passion with everyone who was privileged to work with him. Peter Eckl our friend, professor from the University of Salzburg, who was our collaborator, research partner and scientific mentor for many years and passed away last year.

Conflicts of Interest: The authors declare no conflict of interest.

Sample Availability: Samples of the compounds **2a–l**, **4**, **5a–h**, **6a–d** are available from the authors.

References

1. The global challenge of cancer. *Nat. Cancer* **2020**, *1*, 1–2. [[CrossRef](#)]
2. Gonzalez, H.; Hagerling, C.; Werb, Z. Roles of the immune system in cancer: From tumor initiation to metastatic progression. *Genes Dev.* **2018**, *32*, 1267–1284. [[CrossRef](#)] [[PubMed](#)]
3. Piotrowski, I.; Kulcenty, K.; Suchorska, W. Interplay between inflammation and cancer. *Rep. Pract. Oncol. Radiother* **2020**, *25*, 422–427. [[CrossRef](#)]
4. Ćipak Gašparović, A. Free Radical Research in Cancer. *Antioxidants (Basel)* **2020**, *9*, 157. [[CrossRef](#)] [[PubMed](#)]
5. Cherkas, A.; Zarkovic, N. 4-Hydroxynonenal in Redox Homeostasis of Gastrointestinal Mucosa: Implications for the Stomach in Health and Diseases. *Antioxidants (Basel)* **2018**, *7*, 118. [[CrossRef](#)]
6. Deng, X.; Nakamura, Y. Cancer Precision Medicine: From Cancer Screening to Drug Selection and Personalized Immunotherapy. *Trends Pharmacol. Sci.* **2017**, *38*, 15–24. [[CrossRef](#)]
7. Milkovic, L.; Zarkovic, N.; Saso, L. Controversy about pharmacological modulation of Nrf2 for cancer therapy. *Redox. Biol.* **2017**, *12*, 727–732. [[CrossRef](#)]
8. Jaganjac, M.; Milkovic, L.; Sunjic, S.B.; Zarkovic, N. The NRF2, Thioredoxin, and Glutathione System in Tumorigenesis and Anticancer Therapies. *Antioxidants (Basel)* **2020**, *9*, 1151. [[CrossRef](#)] [[PubMed](#)]
9. Slivka, M.V.; Korol, N.I.; Fizer, M.M. Fused bicyclic 1,2,4-triazoles with one extra sulfur atom: Synthesis, properties, and biological activity. *J. Heterocycl Chem* **2020**, *57*, 3236–3254. [[CrossRef](#)]
10. Tozkoparan, B.; Gökhan, N.; Aktay, G.; Yeşilada, E.; Ertan, M. 6-Benzylidenethiazolo[3,2-b]-1,2,4-triazole-5(6H)-ones substituted with ibuprofen: Synthesis, characterization and evaluation of anti-inflammatory activity. *Eur. J. Med. Chem.* **2000**, *35*, 743–750. [[CrossRef](#)]
11. Assarzadeh, M.J.; Almasirad, A.; Shafiee, A.; Koopaei, M.N.; Abdollahi, M. Synthesis of new thiazolo[3,2-b][1,2,4]triazole-6(5H)-one derivatives as potent analgesic and anti-inflammatory agents. *Med. Chem. Res.* **2014**, *23*, 948–957. [[CrossRef](#)]
12. Toma, A.; Mogoşan, C.; Vlase, L.; Leonte, D.; Zaharia, V. Heterocycles 39. Synthesis, characterization and evaluation of the anti-inflammatory activity of thiazolo[3,2-b][1,2,4]triazole derivatives bearing pyridin-3/4-yl moiety. *Med. Chem. Res.* **2017**, *26*, 2602–2613. [[CrossRef](#)]
13. Tozkoparan, B.; Gökhan, N.; Küpeli, E.; Yeşilada, E.; Ertan, M. Synthesis, characterization and antiinflammatory-analgesic properties of 6-(alpha-amino-4-chlorobenzyl)thiazolo[3,2-b]-1,2,4-triazol-5-ols. *Arzneimittelforschung* **2004**, *54*, 35–41. [[CrossRef](#)]
14. Trairat, C.; Haroun, M.; Papisarva, A.; Kamoutsis, C.; Petrou, A.; Gavalas, A.; Eleftheriou, P.; Geronikaki, A.; Venugopala, K.N.; Kochkar, H.; et al. New Substituted 5-Benzylideno-2-Adamantylthiazol[3,2-b][1,2,4]Triazol-6(5H)ones as Possible Anti-Inflammatory Agents. *Molecules* **2021**, *26*, 659. [[CrossRef](#)] [[PubMed](#)]
15. Barbuceanu, S.F.; Draghici, C.; Barbuceanu, F.; Bancescu, G.; Saramet, G. Design, Synthesis, Characterization and Antimicrobial Evaluation of Some Heterocyclic Condensed Systems with Bridgehead Nitrogen from Thiazolotriazole Class. *Chem. Pharm. Bull. (Tokyo)* **2015**, *63*, 694–700. [[CrossRef](#)]

16. Tratrát, C.; Haroun, M.; Páparisva, A.; Geronikaki, A.; Kamoutsis, Ch.; Ćirić, A.; Glamočlija, J.; Soković, M.; Fotakis, Ch.; Zoumpoulakis, P.; et al. Design, synthesis and biological evaluation of new substituted 5-benzylideno-2-adamantylthiazolo[3,2-b][1,2,4]triazol-6(5H)ones. Pharmacophore models for antifungal activity. *Arab. J. Chem.* **2018**, *11*, 573–590. [[CrossRef](#)]
17. Djukic, M.; Fesatidou, M.; Xenikakis, I.; Geronikaki, A.; Angelova, V.T.; Savic, V.; Pasic, M.; Krilovic, B.; Djukic, D.; Gobeljic, B.; et al. In vitro antioxidant activity of thiazolidinone derivatives of 1,3-thiazole and 1,3,4-thiadiazole. *Chem. Biol. Interact.* **2018**, *286*, 119–131. [[CrossRef](#)]
18. Vijaya Raj, K.K.; Narayana, B. The One Step Synthesis of 2-(2-Bromo-5-methoxyphenyl)-5-(3-arylidene)-1,3-thiazolo[3,2-b]-1,2,4-triazol-6-(5H)-ones and the Evaluation of the Anticonvulsant Activity. *Phosphorus Sulfur Silicon Relat. Elem.* **2006**, *181*, 1971–1981. [[CrossRef](#)]
19. Deng, X.Q.; Song, M.X.; Gong, G.H.; Wang, S.B.; Quan, Z.S. Synthesis and Anticonvulsant Evaluation of some New 6-(Substituted-phenyl)thiazolo[3,2-b][1,2,4]triazole Derivatives in Mice. *Iran. J. Pharm. Res.* **2014**, *13*, 459–469. [[PubMed](#)]
20. Foks, H.; Czarnocka-Janowicz, A.; Rudnicka, W.; Damasiewicz, B.; Nasal, A. Synthesis and biological activity of thiazolo-1,2,4-triazoles. *Acta Pol. Pharm.* **1995**, *52*, 415–420. [[PubMed](#)]
21. Tozkoparan, B.; Akgün, H.; Ertan, M.; Rübsemann, K. Synthesis of some thiazolo[3,2-b]-1,2,4-triazole-5(6H)-ones as potential platelet aggregation inhibitors. *Arch. Pharm. (Weinheim)* **1995**, *328*, 169–173. [[CrossRef](#)]
22. Berk, B.; Aktay, G.; Yesilada, E.; Ertan, M. Synthesis and pharmacological activities of some new 2-[1-(6-methoxy-2-naphthyl)ethyl]-6-(substituted)benzylidene thiazolo[3,2-b]-1,2,4-triazole-5(6H)-one derivatives. *Pharmazie* **2001**, *56*, 613–616. [[CrossRef](#)] [[PubMed](#)]
23. Doğdaş, E.; Tozkoparan, B.; Kaynak, F.B.; Eriksson, L.; Küpeli, E.; Yeşilada, E.; Ertan, M. Design and synthesis of some new thiazolo[3,2-b]-1,2,4-triazole-5(6H)-ones substituted with flurbiprofen as anti-inflammatory and analgesic agents. *Arzneimittelforschung* **2007**, *57*, 196–202. [[CrossRef](#)] [[PubMed](#)]
24. Uzgören-Baran, A.; Tel, B.C.; Sarıgöl, D.; Öztürk, E.İ.; Kazkayası, I.; Okay, G.; Ertan, M.; Tozkoparan, B. Thiazolo[3,2-b]-1,2,4-triazole-5(6H)-one substituted with ibuprofen: Novel non-steroidal anti-inflammatory agents with favorable gastrointestinal tolerance. *Eur. J. Med. Chem.* **2012**, *57*, 398–406. [[CrossRef](#)]
25. Dong, G.; Sheng, C.; Wang, S.; Miao, Z.; Yao, J.; Zhang, W. Selection of evodiamine as a novel topoisomerase I inhibitor by structure-based virtual screening and hit optimization of evodiamine derivatives as antitumor agents. *J. Med. Chem.* **2010**, *53*, 7521–7531. [[CrossRef](#)]
26. Sheng, C.; Miao, Z.; Zhang, W. New strategies in the discovery of novel non-camptothecin topoisomerase I inhibitors. *Curr. Med. Chem.* **2011**, *18*, 4389–4409. [[CrossRef](#)]
27. Reynisson, J.; Court, W.; O'Neill, C.; Day, J.; Patterson, L.; McDonald, E.; Workman, P.; Katan, M.; Eccles, S.A. The identification of novel PLC-gamma inhibitors using virtual high throughput screening. *Bioorg. Med. Chem.* **2009**, *17*, 3169–3176. [[CrossRef](#)]
28. Eurtivong, C.; Pilkington, L.I.; van Rensburg, M.; White, R.M.; Brar, H.K.; Rees, S.; Paulin, E.K.; Xu, C.S.; Sharma, N.; Leung, I.K.H.; et al. Discovery of novel phosphatidylcholine-specific phospholipase C drug-like inhibitors as potential anticancer agents. *Eur. J. Med. Chem.* **2020**, *187*, 111919. [[CrossRef](#)]
29. Lesyk, R.; Vladzimirská, O.; Holota, S.; Zaprutko, L.; Gzella, A. New 5-substituted thiazolo[3,2-b][1,2,4]triazol-6-ones: Synthesis and anticancer evaluation. *Eur. J. Med. Chem.* **2007**, *42*, 641–648. [[CrossRef](#)]
30. Feng, L.; Reynisdóttir, I.; Reynisson, J. The effect of PLC-γ2 inhibitors on the growth of human tumour cells. *Eur. J. Med. Chem.* **2012**, *54*, 463–469. [[CrossRef](#)] [[PubMed](#)]
31. Holota, S.M.; Derkach, H.O.; Demchuk, I.L.; Vynnytska, R.B.; Antoniv, O.I.; Furdychko, L.O.; Slyvka, N.Yu.; Nektegayev, I.O.; Lesyk, R.B. Synthesis and in vivo evaluation of pyrazoline-thiazolidin-4-one hybrid Les-5581 as a potential non-steroidal anti-inflammatory agent. *Biopolym. Cell* **2019**, *35*, 437–447. [[CrossRef](#)]
32. Holota, S.M.; Derkach, G.O.; Zasadko, V.V.; Trokhymchuk, V.V.; Furdychko, L.O.; Demchuk, I.L.; Semenciv, G.M.; Soronovych, I.I.; Kutsyk, R.V.; Lesyk, R.B. Features of antimicrobial activity of some 5-aminomethylene-2-thioxo-4-thiazolidinones. *Biopolym. Cell* **2019**, *35*, 371–380. [[CrossRef](#)]
33. Schadich, E.; Kryshchshyn-Dylevych, A.; Holota, S.; Polishchuk, P.; Džubak, P.; Gurska, S.; Hajdych, M.; Lesyk, R. Assessing different thiazolidine and thiazole based compounds as antileishmanial scaffolds. *Bioorg. Med. Chem. Lett.* **2020**, *30*, 127616. [[CrossRef](#)]
34. Lozynskyi, A.; Holota, S.; Yushyn, I.; Sabadakh, O.; Karpenko, O.; Novikov, V.; Lesyk, R. Synthesis and Biological Activity Evaluation of Polyfunctionalized Anthraquinonehydrazones. *Lett. Drug Des. Discov.* **2021**, *18*, 2. [[CrossRef](#)]
35. Holota, S.; Shylych, Ya.; Derkach, H.; Karpenko, O.; Gzella, A.; Lesyk, R. Synthesis of 4-(2H-[1,2,4]-Triazol-5-ylsulfanyl)-1,2-dihydropyrazol-3-one via Ring-Switching Hydrazinolysis of 5-Ethoxymethylidene-thiazolo[3,2-b][1,2,4]triazol-6-one. *Molbank* **2018**, *4*, M1022. [[CrossRef](#)]
36. Allen, F.H.; Kennard, O.; Watson, D.G.; Brammer, L.; Orpen, A.G.; Taylor, R. Tables of Bond Lengths determined by X-Ray and Neutron Diffraction. Part 1. Bond Lengths in Organic Compounds. *J. Chem. Soc. Perkin. Trans.* **1987**, *2*, S1–19. [[CrossRef](#)]
37. Monks, A.; Scudiero, D.; Skehan, P.; Shoemaker, R.; Paull, K.; Vistica, D.; Hose, C.; Langley, J.; Cronise, P.; Vaigro-Wolff, A.; et al. Feasibility of a high-flux anticancer drug screen using a diverse panel of cultured human tumor cell lines. *J. Natl. Cancer Inst.* **1991**, *83*, 757–766. [[CrossRef](#)] [[PubMed](#)]
38. Boyd, M.R.; Paull, K.D. Some Practical Considerations and Applications of the National Cancer Institute in Vitro Anticancer Drug Discovery Screen. *Drug Dev. Res.* **1995**, *34*, 91–109. [[CrossRef](#)]

39. Boyd, M.R. The NCI In Vitro Anticancer Drug Discovery Screen. In *Anticancer Drug Development Guide*; Teicher, B.A., Ed.; Humana Press: Totowa, NJ, USA, 1997; Volume 2, pp. 23–42. [[CrossRef](#)]
40. Shoemaker, R.H. The NCI60 human tumour cell line anticancer drug screen. *Nat. Rev. Cancer* **2006**, *6*, 813–823. [[CrossRef](#)] [[PubMed](#)]
41. Holbeck, S.L. Update on NCI in vitro drug screen utilities. *Eur. J. Cancer* **2004**, *40*, 785–793. [[CrossRef](#)] [[PubMed](#)]
42. Holbeck, S.L.; Collins, J.M.; Doroshow, J.H. Analysis of Food and Drug Administration-approved anticancer agents in the NCI60 panel of human tumor cell lines. *Mol. Cancer Ther.* **2010**, *9*, 1451–1460. [[CrossRef](#)] [[PubMed](#)]
43. Grange, E.W.; Henry, D.W.; Lee, W.W. Glyoxylic Acid Hydrocarbonylsulfonylhydrazones and Therapeutic Compositions. U.S. Patent US4218465A, 19 August 1980.
44. Pretzer, D.; Repta, A.J. Stability of the experimental anticancer agent [(4-methoxyphenyl)sulfonyl]hydrazono]acetic acid (NSC-267213). I. Kinetics and mechanism of degradation. *Int. J. Pharm.* **1987**, *38*, 147–160. [[CrossRef](#)]
45. Pretzer, D.; Repta, A.J. Stability of the experimental anticancer agent [(4-methoxyphenyl) sulfonyl] hydrazono] acetic acid (NSC-267213). II. Effect of structural modification on stability and mechanism of degradation. *Int. J. Pharm.* **1987**, *38*, 161–169. [[CrossRef](#)]
46. Shyam, K.; Cosby, L.A.; Sartorelli, A.C. Relationship between structure and antineoplastic activity of (arylsulfonyl)hydrazones of 4-pyridinecarboxaldehyde. *J. Med. Chem.* **1985**, *28*, 149–152. [[CrossRef](#)]
47. Morgan, D.M. Tetrazolium (MTT) assay for cellular viability and activity. *Methods Mol. Biol.* **1998**, *79*, 179–183. [[CrossRef](#)]
48. Ainsworth, C. 1,2,4-Triazole. *Org. Synth.* **1960**, *40*, 99. [[CrossRef](#)]
49. *Rigaku Oxford Diffraction, CrysAlis-Pro Software System*; Version 1.171.38.41; Rigaku Corporation: Oxford, UK, 2015.
50. Sheldrick, G.M. SHELXT-Integrated space-group and crystal-structure determination. *Acta Cryst. A* **2015**, *71*, 3–8. [[CrossRef](#)] [[PubMed](#)]
51. Sheldrick, G.M. Crystal structure refinement with SHELXL. *Acta Cryst.* **2015**, *C71*, 3–8. [[CrossRef](#)]
52. Farrugia, L.J. WinGX and ORTEP for windows: An update. *J. Appl. Cryst.* **2012**, *45*, 849–854. [[CrossRef](#)]
53. Dolomanov, O.V.; Bourhis, L.J.; Gildea, R.J.; Howard, J.A.K.; Puschmann, H. OLEX2: A complete structure solution, refinement and analysis program. *J. Appl. Cryst.* **2009**, *42*, 339–341. [[CrossRef](#)]
54. Spek, A.L. Structure validation in chemical crystallography. *Acta Cryst.* **2009**, *65*, 148–155. [[CrossRef](#)] [[PubMed](#)]
55. Chen, Y.F.; Lin, Y.C.; Morris-Natschke, S.L.; Wei, C.F.; Shen, T.C.; Lin, H.Y.; Hsu, M.H.; Chou, L.C.; Zhao, Y.; Kuo, S.C.; et al. Synthesis and SAR studies of novel 6,7,8-substituted 4-substituted benzyloxyquinolin-2(1H)-one derivatives for anticancer activity. *Br. J. Pharmacol.* **2015**, *172*, 1195–1221. [[CrossRef](#)] [[PubMed](#)]